

ANALYSIS OF CAPSULE R FROM THE WISCONSIN PUBLIC
SERVICE CORPORATION KEWAUNEE NUCLEAR PLANT
REACTOR VESSEL RADIATION SURVEILLANCE PROGRAM
(WCAP-9878)

EPRI RESEARCH PROJECT 1021-3
TOPICAL REPORT

March 1981

Prepared by

WESTINGHOUSE ELECTRIC CORPORATION

Nuclear Technology Division

P. O. Box 355

Pittsburgh, Pennsylvania 15230

T. R. Mager, Principal Investigator

Prepared for

ELECTRIC POWER RESEARCH INSTITUTE

3412 Hillview Avenue

Palo Alto, California 94304

T. U. Marston, Project Manager

**ANALYSIS OF CAPSULE R FROM THE WISCONSIN PUBLIC
SERVICE CORPORATION KEWAUNEE NUCLEAR PLANT
REACTOR VESSEL RADIATION SURVEILLANCE PROGRAM
(WCAP-9878)**

**EPRI RESEARCH PROJECT 1021-3
TOPICAL REPORT**

S. E. Yanichko
S. L. Anderson
R. P. Shogan
R. G. Lott

March 1981

Prepared by

WESTINGHOUSE ELECTRIC CORPORATION
Nuclear Technology Division
P. O. Box 355
Pittsburgh, Pennsylvania 15230
T. R. Mager, Principal Investigator

Prepared for

ELECTRIC POWER RESEARCH INSTITUTE
3412 Hillview Avenue
Palo Alto, California 94304
T. U. Marston, Project Manager

LEGAL NOTICE

This report was prepared by Westinghouse Electric Corporation (WESTINGHOUSE) as an account of work sponsored by the Electric Power Research Institute, Inc. (EPRI). Neither EPRI, members of EPRI, nor WESTINGHOUSE, nor any person acting on behalf of either:

- a. Makes any warranty or representation, express or implied, with respect to the accuracy, completeness, or usefulness of the information contained in this report, or that the use of any information, apparatus, method, or process disclosed in this report may not infringe privately owned rights; or
- b. Assumes any liabilities with respect to the use of, or for damages resulting from the use of, any information, apparatus, method, or process disclosed in this report.

TABLE OF CONTENTS

Section	Title	Page
1	SUMMARY OF RESULTS	1-1
2	INTRODUCTION	2-1
3	BACKGROUND	3-1
4	DESCRIPTION OF PROGRAM	4-1
5	TESTING OF SPECIMENS FROM CAPSULE R	5-1
	5-1. Overview	5-1
	5-2. Charpy V-Notch Impact Test Results	5-2
	5-3. Tensile Test Results	5-24
	5-4. Wedge Opening Loading Tests	5-32
6	RADIATION ANALYSIS AND NEUTRON DOSIMETRY	6-1
	6-1. Introduction	6-1
	6-2. Discrete Ordinates Analysis	6-1
	6-3. Neutron Dosimetry	6-6
	6-4. Transport Analysis Results	6-10
	6-5. Dosimetry Results	6-18
References		A-1

LIST OF ILLUSTRATIONS

Figure	Title	Page
4-1	Arrangement of Surveillance Capsules in Kewaunee Reactor Vessel (Updated Lead Factors for the Capsules Are Shown in Parentheses)	4-2
4-2	Schematic Diagram of Capsule 24 Showing Location of Specimens, Thermal Monitors, and Dosimeters	4-3
5-1	Charpy V-Notch Impact Data for Kewaunee Reactor Vessel Shell Forging 122X208VA1	5-6
5-2	Charpy V-Notch Impact Data for Kewaunee Reactor Vessel Shell Forging 123X167VA1	5-7
5-3	Charpy V-Notch Impact Data for Kewaunee Reactor Vessel Weld Metal	5-8
5-4	Charpy V-Notch Impact Data for Kewaunee Reactor Vessel Weld HAZ Metal	5-9
5-5	Charpy V-Notch Impact Data for A533 Grade B Class 1 ASTM Correlation Monitor Material	5-10
5-6	Charpy Impact Specimen Fracture Surfaces for Kewaunee Intermediate Shell Forging 122X208VA1	5-19
5-7	Charpy Impact Specimen Fracture Surfaces for Kewaunee Lower Shell Forging 123X167VA1	5-20
5-8	Charpy Impact Specimen Fracture Surfaces for Kewaunee Weld Metal	5-21
5-9	Charpy Impact Specimen Fracture Surfaces for Kewaunee HAZ Material	5-22
5-10	Charpy Impact Specimen Fracture Surfaces for Kewaunee ASTM Correlation Monitor Material	5-23

LIST OF ILLUSTRATIONS (cont)

Figure	Title	Page
5-11	Comparison of Predicted Versus Actual 41-Joule Transition Temperature Increases for Kewaunee Reactor Vessel Materials	5-26
5-12	Tensile Properties for Kewaunee Reactor Vessel Shell Forging 122X208VA1	5-29
5-13	Tensile Properties for Kewaunee Reactor Vessel Shell Forging 123X167VA1	5-30
5-14	Tensile Properties for Kewaunee Reactor Vessel Weld Metal	5-31
5-15	Typical Stress-Strain Curve for Tension Specimens	5-33
5-16	Fractured Tensile Specimens From Kewaunee Intermediate Shell Forging 122X208VA1	5-34
5-17	Fractured Tensile Specimens From Kewaunee Lower Shell Forging 123X167VA1	5-35
5-18	Fractured Tensile Specimens From Kewaunee Weld Metal	5-36
6-1	Kewaunee Reactor Geometry	6-2
6-2	Plan View of a Reactor Vessel Surveillance Capsule	6-4
6-3	Calculated Azimuthal Distribution of Maximum Fast Neutron Flux ($E > 1$ Mev) Within the Pressure Vessel Surveillance Capsule Geometry	6-11
6-4	Calculated Radial Distribution of Maximum Fast Neutron Flux ($E > 1$ Mev) Within the Pressure Vessel	6-12

LIST OF ILLUSTRATIONS (cont)

Figure	Title	Page
6-5	Relative Axial Variation of Fast Neutron Flux ($E > 1.0$ Mev) Within the Pressure Vessel	6-13
6-6	Calculated Radial Distribution of Maximum Fast Neutron Flux ($E > 1$ Mev) Within the Surveillance Capsules	6-14
6-7	Calculated Variation of Fast Neutron Flux Monitor Saturated Activity Within Capsules V and R	6-15
6-8	Comparison of Measured and Calculated Fast Neutron Fluence ($E > 1$ Mev) for Capsules V and R	6-27

LIST OF TABLES

Table	Title	Page
4-1	Chemistry and Heat Treatment of Material Representing the Core Region Shell Forgings and Weld Metal From Kewaunee Reactor Vessel	4-5
4-2	Chemistry and Heat Treatment of Surveillance Material Representing 12-Inch-Thick A533 Grade B Class 1 ASTM Correlation Monitor Material From HSST Plate 02	4-6
5-1	Charpy Impact Data for Kewaunee Reactor Pressure Vessel Shell Forgings	5-3
5-2	Charpy Impact Data for Kewaunee Reactor Pressure Vessel Weld Metal and HAZ Material	5-4
5-3	Charpy Impact Data for the ASTM Correlation Monitor Material (HSST Plate 02)	5-5
5-4	Instrumented Charpy Impact Test Results for Kewaunee Shell Forgings	5-11
5-5	Instrumented Charpy Impact Test Results for Kewaunee Weld Metal and HAZ Material	5-13
5-6	Instrumented Charpy Impact Test Results for the ASTM Correlation Monitor Material	5-15
5-7	The Effect of 288°C Irradiation to $2.07 \times 10^{19} \text{ n/cm}^2$ ($E > 1 \text{ Mev}$) on the Notch Toughness Properties of Kewaunee Reactor Vessel Surveillance Test Material	5-17
5-8	Summary of Kewaunee Reactor Vessel Surveillance Capsule Charpy Impact Test Results	5-25
5-9	Tensile Properties for Kewaunee Reactor Vessel Material Irradiated to $2.07 \times 10^{19} \text{ n/cm}^2$ ($E > 1 \text{ Mev}$)	5-27

LIST OF TABLES (cont)

Table	Title	Page
6-1	21 Group Energy Structure	6-5
6-2	Nuclear Parameters for Neutron Flux Monitors	6-7
6-3	Calculated Fast Neutron Flux ($E > 1$ Mev) and Lead Factors for Kewaunee Surveillance Capsules	6-16
6-4	Calculated Neutron Energy Spectra at the Center of Kewaunee Surveillance Capsules	6-17
6-5	Spectrum Averaged Reaction Cross Sections at the Dosimeter Block Location for Kewaunee Surveillance Capsules	6-18
6-6	Irradiation History of Kewaunee Reactor Vessel Surveillance Capsules	6-19
6-7	Comparison of Measured and Calculated Fast Neutron Flux Monitor Saturated Activities for Capsule V	6-22
6-8	Comparison of Measured and Calculated Fast Neutron Flux Monitor Saturated Activities for Capsule R	6-23
6-9	Results of Fast Neutron Dosimetry for Capsules V and R	6-25
6-10	Results of Thermal Neutron Dosimetry for Capsules V and R	6-26
6-11	Summary of Fast Neutron Dosimetry Results Capsules V and R	6-28

SECTION 1

SUMMARY OF RESULTS

The analyses of the reactor vessel material contained in the second surveillance capsule, designated R from the Wisconsin Public Service Corporation Kewaunee nuclear plant reactor pressure vessel, led to the following conclusions:

- The capsule received an average fast fluence of $2.07 \times 10^{19} \text{ n/cm}^2$ ($E > 1 \text{ Mev}$) compared to a calculated value of $2.06 \times 10^{19} \text{ n/cm}^2$.
- Based on the fluence measurements for Capsule R, the vessel 1/4 thickness fluence after 4.5 effective full power years of operation is $3.77 \times 10^{18} \text{ n/cm}^2$ compared to a calculated fluence of $3.75 \times 10^{18} \text{ n/cm}^2$.
- Results of Charpy impact tests for the two Kewaunee capsules tested to date indicate that radiation damage has not saturated.
- End-of-life projected fast neutron fluences for the reactor vessel, based on 32 full-power years of operation at 1650 MW, are as follows:

Vessel Location	Fast Neutron Fluence (n/cm^2)	
	Calculated	Measured
Inner surface	4.34×10^{19}	4.47×10^{19}
1/4 thickness	2.83×10^{19}	2.91×10^{19}
3/4 thickness	8.53×10^{18}	8.78×10^{18}

SECTION 2

INTRODUCTION

This report presents the results of the examination of Capsule R, the second capsule of the continuing surveillance program which monitors the effects of neutron irradiation on the Wisconsin Public Service Corporation Kewaunee Nuclear Plant reactor pressure vessel materials under actual operating conditions.

The surveillance program for the Kewaunee reactor pressure vessel materials was designed and recommended by the Westinghouse Electric Corporation. A description of the surveillance program and the preirradiation mechanical properties of the reactor vessel materials are presented in WCAP-8017.^[1] The surveillance program was planned to cover the 40-year life of the reactor pressure vessel and was based on ASTM E-185-70, "Recommended Practice for Surveillance Tests for Nuclear Reactor Vessels."^[2]

This report summarizes testing and the postirradiation data obtained from the second material surveillance capsule (Capsule R) removed from the Kewaunee reactor vessel and discusses the analysis of these data. The data are also compared to results of the previously removed Kewaunee Capsule V, reported in WCAP-8908.^[3]

SECTION 3

BACKGROUND

The ability of the large steel pressure vessel containing the reactor core and its primary coolant to resist fracture constitutes an important factor in ensuring safety in the nuclear industry. The beltline region of the reactor pressure vessel is the most critical region of the vessel because it is subjected to significant fast neutron bombardment. The overall effects of fast neutron irradiation on the mechanical properties of low alloy ferritic pressure vessel steels such as A508 Class 2 (base material of the Kewaunee reactor pressure vessel beltline) are well documented in the literature. Generally, low alloy ferritic materials show an increase in hardness and tensile properties and a decrease in ductility and toughness under certain conditions of irradiation.

A method for performing analyses to guard against fast fracture in reactor pressure vessels has been presented in "Protection Against Nonductile Failure," Appendix G, to Section III of the ASME Boiler and Pressure Vessel Code. The method utilizes fracture mechanics concepts and is based on the reference nil-ductility temperature, RT_{NDT} .

RT_{NDT} is defined as the greater of the drop weight nil-ductility transition temperature (NDTT per ASTM E-208) or the temperature 60°F less than the 50 ft lb temperature (or 35-mil lateral expansion if this is greater) temperature as determined from Charpy specimens oriented normal to the working direction of the material. The RT_{NDT} of a given material is used to index that material to a reference stress intensity factor curve (K_{IR} curve) which appears in Appendix G of the ASME Code. The K_{IR} curve is a lower bound of dynamic, crack arrest, and static fracture toughness results obtained from several heats of pressure vessel steel. When a given material is indexed to the K_{IR} curve, allowable stress intensity factors can be obtained for this material as a function of temperature. Allowable operating limits can then be determined utilizing these allowable stress intensity factors.

RT_{NDT} and, in turn, the operating limits of nuclear power plants can be adjusted to account for the effects of radiation on the reactor vessel material properties. The radiation embrittlement or changes in mechanical properties of a given reactor pressure vessel steel can be monitored by a reactor surveillance program such as the Kewaunee Reactor Vessel Radiation Surveillance Program,^[1] in which a surveillance capsule is periodically removed from the operating nuclear

reactor and the encapsulated specimens are tested. The increase in the Charpy V-notch 50 ft lb temperature (ΔRT_{NDT}) due to irradiation is added to the original RT_{NDT} to adjust the RT_{NDT} for radiation embrittlement. This adjusted RT_{NDT} (RT_{NDT} initial + ΔRT_{NDT}) is used to index the material to the K_{IR} curve and, in turn, to set operating limits for the nuclear power plant which take into account the effects of irradiation on the reactor vessel materials.

SECTION 4

DESCRIPTION OF PROGRAM

Six surveillance capsules for monitoring the effects of neutron exposure on the Kewaunee reactor pressure vessel core region material were inserted in the reactor vessel prior to initial plant startup. The six capsules were positioned in the reactor vessel between the thermal shield and the vessel wall at locations shown in figure 4-1. The vertical center of the capsules is opposite the vertical center of the core.

Capsule R was removed after 4.5 effective full power years of plant operation. This capsule contained Charpy V-notch impact, tensile, and WOL specimens (figure 4-2) from the intermediate and lower shell ring forgings and weld metal representative of the core region of the reactor vessel and Charpy V-notch specimens from weld heat-affected zone (HAZ) material. The capsule also contained Charpy V-notch specimens from the 12-inch-thick ASTM correlation monitor material (A533 Grade B Class 1). The chemistry and heat treatment of the surveillance material are presented in tables 4-1 and 4-2.

All test specimens were machined from the 1/4 thickness location of the forgings. Test specimens represent material taken at least one forging thickness from the quenched end of the forging. All base metal Charpy V-notch and tensile specimens were oriented with the longitudinal axis of the specimen parallel to the principal working direction of the forgings. The WOL test specimens were machined with the simulated crack of the specimen perpendicular to the surfaces and rolling direction of the forgings.

Charpy V-notch specimens from the weld metal were oriented with the longitudinal axis of the specimens transverse to the welding direction. Tensile specimens were oriented with the longitudinal axis of the specimen parallel to the welding direction.

Capsule R contained dosimeter wires of pure iron, copper, nickel, and aluminum-cobalt (cadmium-shielded and unshielded). In addition, cadmium-shielded dosimeters of Np^{237} and U^{238} were contained in the capsule and located as shown in figure 4-2.

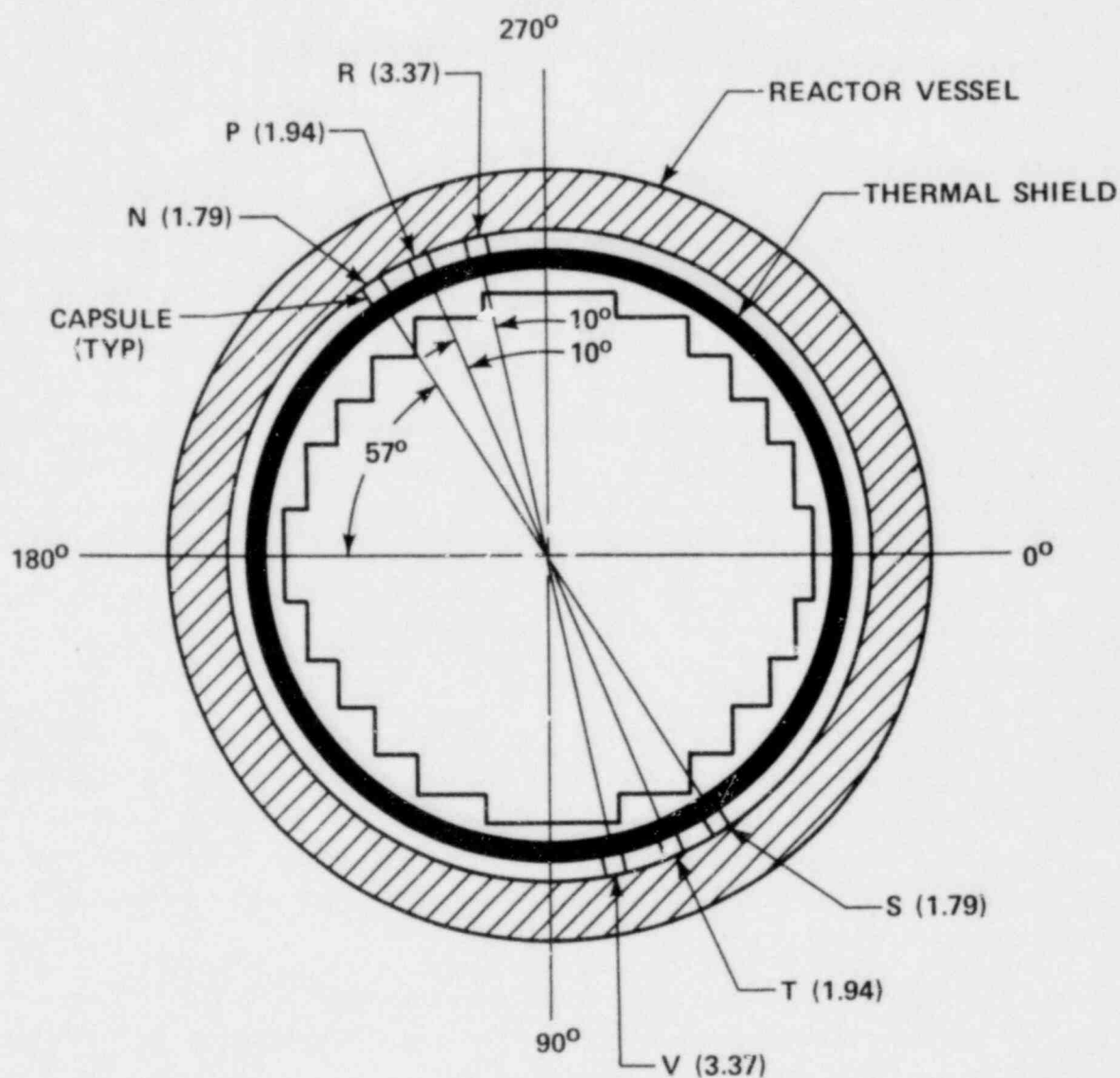
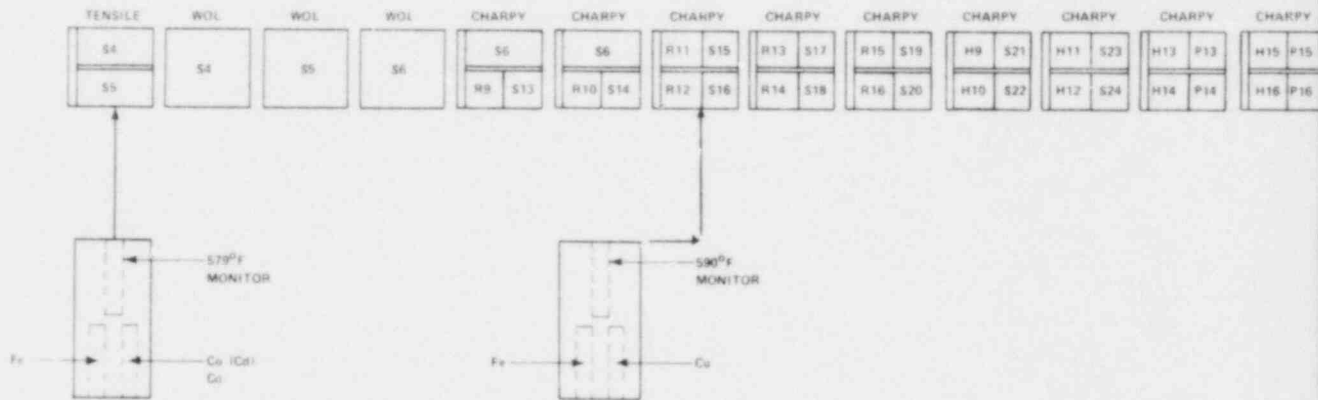


Figure 4-1. Arrangement of Surveillance Capsules in Kewaunee Reactor Vessel (Updated Lead Factors for the Capsules Are Shown in Parentheses)

TENSILE



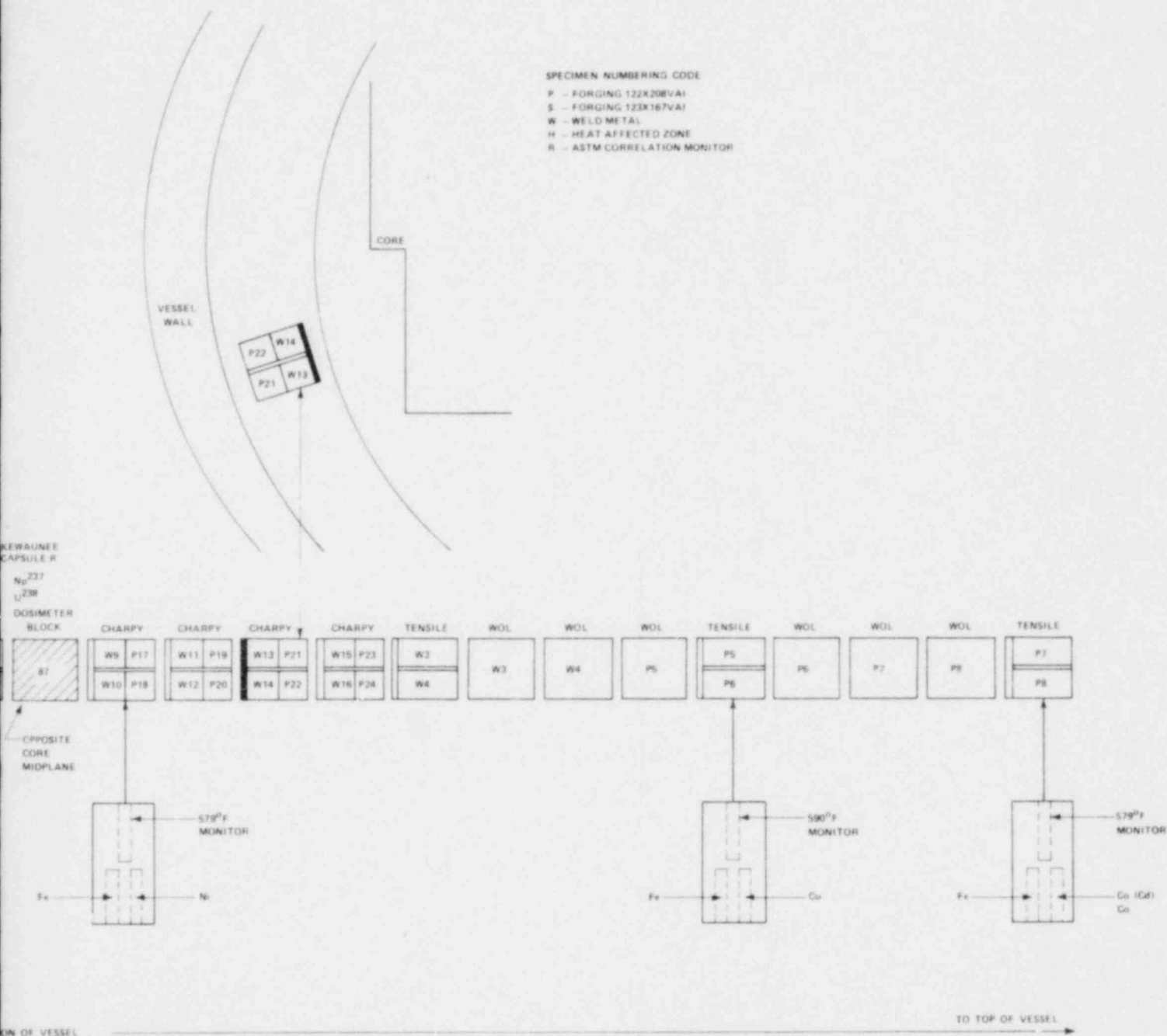


Figure 4-2. Schematic Diagram of Capsule R Showing Location of Specimens, Thermal Monitors, and Dosimeters

TABLE 4-1

**CHEMISTRY AND HEAT TREATMENT OF MATERIAL REPRESENTING THE
CORE REGION SHELL FORGINGS AND WELD METAL FROM
KEWAUNEE REACTOR VESSEL**

Element	CHEMICAL ANALYSIS (wt %)		
	Forging 122X208VA1	Forging 123X167VA1	Weld Metal
C	0.21	0.20	0.12
Si	0.25	0.28	0.20
Mo	0.58	0.58	0.48
Cu	0.06	0.06	0.20
Ni	0.71	0.75	0.77
Mn	0.69	0.79	1.37
Cr	0.40	0.35	0.090
V	<0.02	<0.02	0.002
Co	0.011	0.012	0.001
Sn	0.01	0.01	0.004
Ti	<0.001	<0.001	<0.001
Zr	0.001	0.001	<0.001
As	0.001	0.004	0.004
Sb	<0.001	0.001	0.001
S	0.011	0.009	0.011
P	0.010	0.010	0.016
Al	0.004	0.006	0.010
B	<0.003	<0.003	<0.003
N ₂	0.006	0.010	0.012
Zn	—	—	<0.001
HEAT TREATMENT			
Intermediate Shell	Heated at 1550°F for 8 hours, water-quenched		
Forging Heat 122X208VA1	Tempered at 1230°F for 14 hours, air-cooled		
	Stress-relieved at 1150°F for 21 hours, furnace-cooled		
Lower Shell Forging	Heated at 1550°F for 8 hours, water-quenched		
Heat 123X167VA1	Tempered at 1220°F for 14 hours, air-cooled		
	Stress-relieved at 1150°F for 21 hours, furnace-cooled		
Submerged Arc Weldment	Stress-relieved at 1150°F for 19-1/4 hours, furnace-cooled		

TABLE 4-2

CHEMISTRY AND HEAT TREATMENT OF SURVEILLANCE MATERIAL
REPRESENTING 12-INCH-THICK A533 GRADE B CLASS 1
ASTM CORRELATION MONITOR MATERIAL FROM HSST PLATE 02

Chemical Analysis (wt %)							
C	Mn	P	S	Si	Ni	Mo	Cu
0.22	1.48	0.012	0.018	0.25	0.68	0.52	0.14
Heat Treatment							
Heated at $1675 \pm 25^{\circ}\text{F}$ — 4 hours — air-cooled							
Heated at $1600 \pm 25^{\circ}\text{F}$ — 4 hours — water-quenched							
Tempered at $1225 \pm 25^{\circ}\text{F}$ — 4 hours — furnace-cooled							
Stress-relieved at $1150 \pm 25^{\circ}\text{F}$ — 40 hours — furnace-cooled to 600°F							

Thermal monitors made from two low-melting eutectic alloys and sealed in Pyrex tubes were included in the capsule and were located as shown in figure 4-2. The two eutectic alloys and their melting points are:

2.5 Ag, 97.5 Pb

Melting Point 579°F (304°C)

1.75 Ag, 0.75 Sn, 97.5 Pb

Melting Point 590°F (310°C)

SECTION 5

TESTING OF SPECIMENS FROM CAPSULE R

5-1. OVERVIEW

The postirradiation mechanical testing of the Charpy V-notch and tensile specimens was performed at the Westinghouse Research and Development Laboratory with consultation by Westinghouse Nuclear Energy Systems personnel. Testing was performed in accordance with 10CFR50, Appendices G and H.

Upon receipt of the capsule at the laboratory, the specimens and spacer blocks were carefully removed, inspected for identification number, and checked against the master list in WCAP-8017.^[1] No discrepancies were found.

Examination of the two low-melting 304°C (579°F) and 310°C (590°F) eutectic alloys indicated no melting of either type of thermal monitor. Based on this examination, the maximum temperature to which the test specimens were exposed was less than 304°C (579°F).

The Charpy impact tests were performed on a Tinius-Olsen Model 74, 358J machine. The tup (striker) of the Charpy machine is instrumented with an Effects Technology model 500 instrumentation system. With this system, load-time and energy-time signals can be recorded in addition to the standard measurement of Charpy energy (E_D). From the load-time curve, the load of general yielding (P_{GY}), the time to general yielding (t_{GY}), the maximum load (P_M), and the time to maximum load (t_M) can be determined. Under some test conditions, a sharp drop in load indicative of fast fracture was observed. The load at which fast fracture was initiated is identified as the fast fracture load (P_F), and the load at which fast fracture terminated is identified as the arrest load (P_A).

The energy at maximum load (E_M) was determined by comparing the energy-time record and the load-time record. The energy at maximum load is roughly equivalent to the energy required to initiate a crack in the specimen. Therefore, the propagation energy for the crack (E_P) is the difference between the total energy to fracture (E_D) and the energy at maximum load.

The yield stress (σ_Y) is calculated from the three point bend formula. The flow stress is calculated from the average of the yield and maximum loads, also using the three point bend formula.

Percent shear was determined from postfracture photographs using the ratio-of areas method in compliance with ASTM Specification A370-74. The lateral expansion was measured using a dial gage rig similar to that shown in the same specification.

Tensile tests were performed on a 20,000-pound Instron, split-console test machine (Model 1115) per ASTM Specifications E8 and E21, and MHL Procedure 7604 Revision 2. All pull rods, grips, and pins were made of Inconel 718 hardened to R_c 45. The upper pull rod was connected through a universal joint to improve axially of loading. The tests were conducted at a constant crosshead speed of 0.05 inch per minute throughout the test.

Deflection measurements were made with a linear variable displacement transducer (LVDT) extensometer. The extensometer knife edges were spring-loaded to the specimen and operated through specimen failure. The extensometer gage length is 1.00 inch. The extensometer is rated as Class B-2 per ASTM E83.

Elevated test temperatures were obtained with a three-zone electric resistance split-tube furnace with a 9-inch hot zone. All tests were conducted in air.

Because of the difficulty in remotely attaching a thermocouple directly to the specimen, the following procedure was used to monitor specimen temperature. Chromel-alumel thermocouples were inserted in shallow holes in the center and each end of the gage section of a dummy specimen and in each grip. In test configuration, with a slight load on the specimen, a plot of specimen temperature versus upper and lower grip and controller temperatures was developed over the range room temperature to 550°F. The upper grip was used to control the furnace temperature. During the actual testing the grip temperatures were used to obtain desired specimen temperatures. Experiments indicated that this method is accurate to plus or minus 2°F.

The yield load, ultimate load, fracture load, total elongation, and uniform elongation were determined directly from the load-extension curve. The yield strength, ultimate strength, and fracture strength were calculated using the original cross-sectional area. The final diameter and final gage length were determined from postfracture photographs. The fracture area used to calculate the fracture stress (true stress at fracture) and percent reduction in area was computed using the final diameter measurement.

5-2. CHARPY V-NOTCH IMPACT TEST RESULTS

The toughness results from Charpy V-notch impact tests performed on the various surveillance materials in Capsule R after irradiation to 2.07×10^{19} n/cm² are presented in tables 5-1 through 5-3 and figures 5-1 through 5-5. Instrumented Charpy impact test results for the various materials are shown in tables 5-4 through 5-6. A summary of the surveillance test results is presented in table 5-7. The fractured surfaces of the impact specimens are shown in figures 5-6 through 5-10.

TABLE 5-1

**CHARPY IMPACT DATA FOR KEWAUNEE REACTOR
PRESSURE VESSEL SHELL FORGINGS**
(Irradiated to 2.07×10^{19} n/cm²)

Sample Number	Temperature		Impact Energy		Lateral Expansion		Shear (%)
	(°C)	(°F)	(J)	(ft lb)	(mm)	(mils)	
Forging 122X208VA1							
P-23	-46	-50	11.0	8.0	0.20	8.0	0
P-16	-32	-25	17.5	13.0	0.25	10.0	0
P-18	-18	0	59.0	43.5	0.94	37.0	17
P-21	-18	0	97.5	72.0	1.50	59.0	28
P-13	-1	30	151.0	111.5	1.93	76.0	54
P-14	26	78	68.5	50.5	1.04	41.0	38
P-17	26	78	170.0	125.5	2.26	89.0	63
P-24	52	125	164.5	121.5	2.16	85.0	78
P-15	93	200	170.0	125.5	2.26	89.0	77
P-20	121	250	228.0	168.0	2.36	93.0	100
P-22	149	300	210.0	155.0	2.31	91.0	100
Forging 123X167VA1							
S-20	-73	-100	9.5	7.0	0.15	6.0	0
S-13	-46	-50	44.5	33.0	0.66	26.0	19
S-19	-32	-25	74.0	54.5	1.09	43.0	17
S-21	-32	-25	77.5	57.0	1.09	43.0	21
S-15	-18	0	35.5	26.0	0.53	21.0	8
S-23	-18	0	77.5	57.0	1.17	46.0	17
S-22	-1	30	131.5	97.0	1.80	71.0	51
S-24	10	50	103.5	76.5	1.45	57.0	38
S-14	16	60	135.5	100.0	1.85	73.0	63
S-18	26	78	221.0	163.0	2.54	100.0	100
S-16	66	150	198.5	146.5	2.44	96.0	100
S-17	93	200	203.5	150.0	2.36	93.0	100

TABLE 5-2

CHARPY IMPACT DATA FOR KEWAUNEE REACTOR
 PRESSURE VESSEL WELD METAL AND HAZ MATERIAL
 (Irradiated to 2.07×10^{19} n/cm²)

Sample Number	Temperature		Impact Energy		Lateral Expansion		Shear (%)
	(°C)	(°F)	(J)	(ft lb)	(mm)	(mils)	
Weld Metal							
W-10	26	78	10.0	7.5	0.30	12.0	19
W-15	66	150	36.0	26.5	0.53	21.0	30
W-11	93	200	42.5	31.5	0.61	24.0	30
W-16	99	210	55.0	40.5	1.04	41.0	50
W-12	107	225	67.0	49.5	1.02	40.0	65
W-9	121	250	106.5	78.5	1.47	58.0	95
W-14	149	300	105.0	77.5	1.63	64.0	100
W-13	177	350	107.0	79.0	1.78	70.0	100
HAZ Material							
H-10	-18	0	21.0	15.5	0.36	14.0	14
H-13	10	50	159.5	117.5	2.08	82.0	69
H-14	26	78	75.0	55.5	1.04	41.0	36
H-11	52	125	67.0	49.5	1.04	41.0	50
H-9	66	150	137.0	101.0	2.03	80.0	76
H-16	93	200	177.0	130.5	2.44	96.0	100
H-12	149	300	218.5	161.0	2.44	96.0	100
H-15	177	350	179.5	132.5	2.49	98.0	100

TABLE 5-3
 CHARPY IMPACT DATA FOR THE ASTM CORRELATION
 MONITOR MATERIAL
 (HSST Plate 02)

Sample Number	Temperature		Impact Energy		Lateral Expansion		Shear (%)
	(°C)	(°F)	(J)	(ft lb)	(mm)	(mils)	
R-13	26	78	10.0	7.5	0.13	5.0	14
R-12	66	150	30.5	22.5	0.48	19.0	25
R-9	93	200	44.0	32.5	0.76	30.0	27
R-10	99	210	50.0	37.0	0.76	30.0	35
R-16	107	225	109.0	80.5	1.40	55.0	70
R-15	121	250	131.5	97.0	1.75	69.0	69
R-11	149	300	122.5	90.5	1.91	75.0	100
R-14	177	350	134.0	99.0	2.36	93.0	100

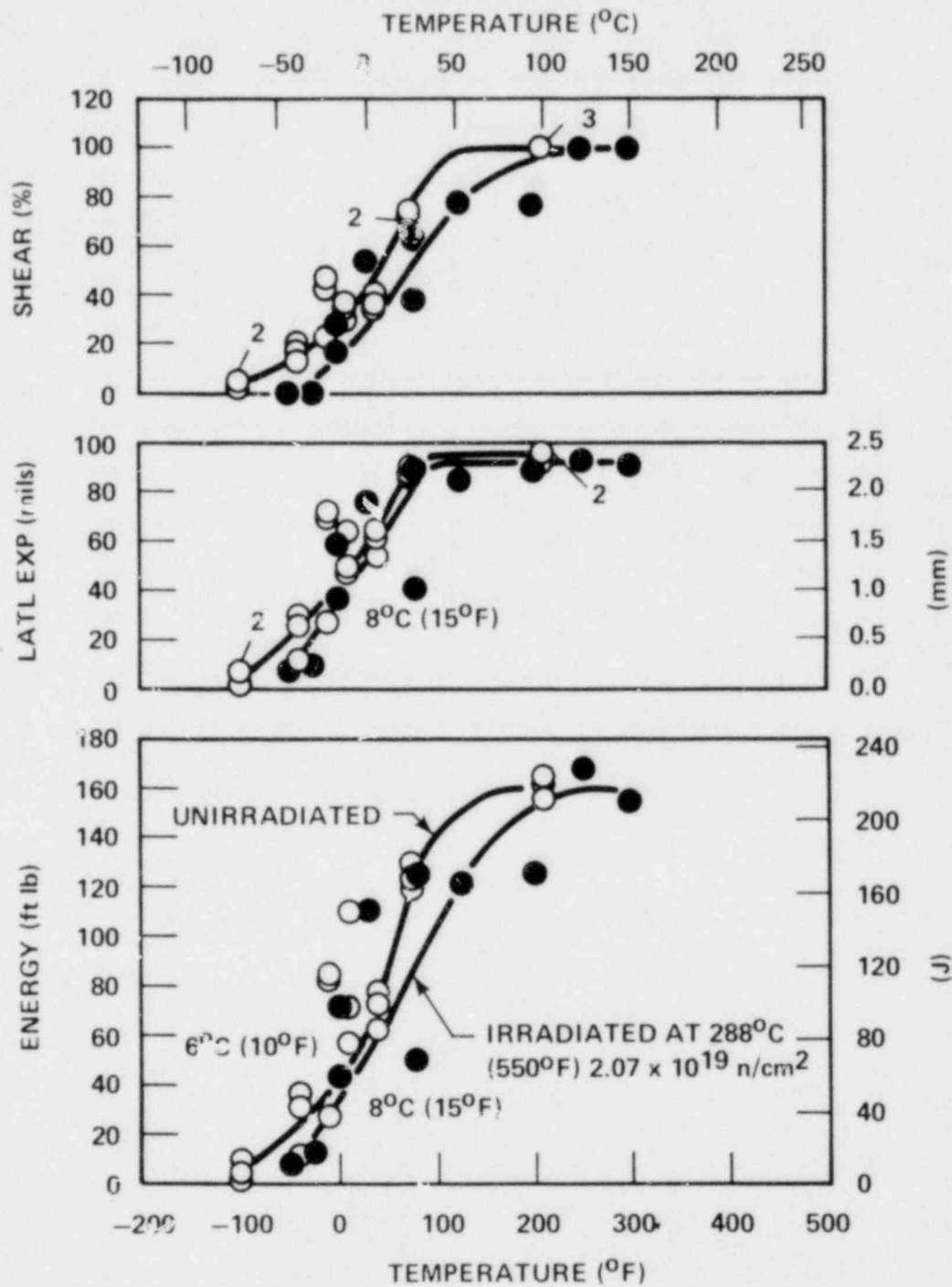


Figure 5-1. Charpy V-Notch Impact Data for Kewaunee Reactor Vessel Shell Forging 122x208 VA1

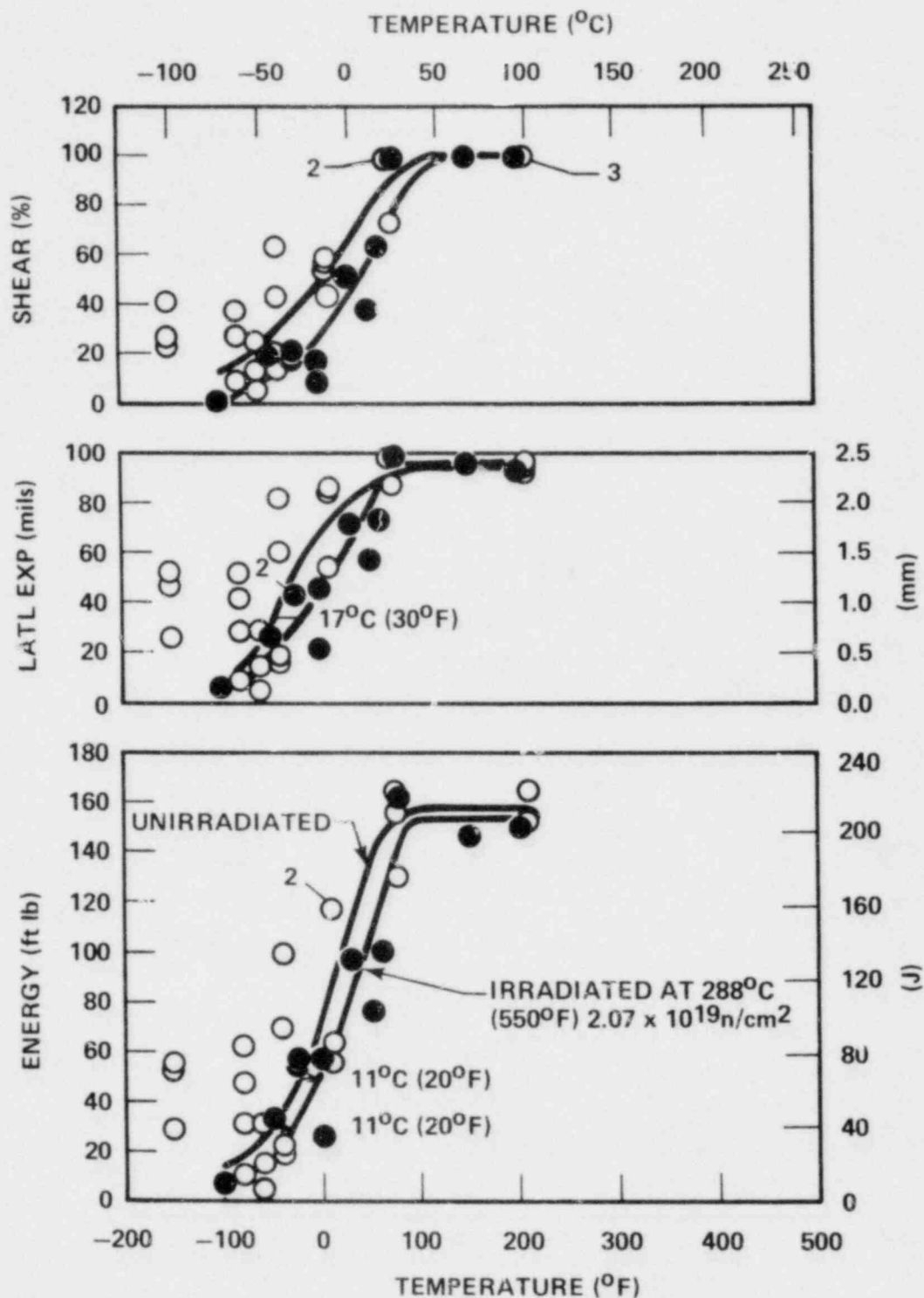


Figure 5-2. Charpy V-Notch Impact Data for Kewaunee Reactor Vessel Shell Forging 123x167 VA1

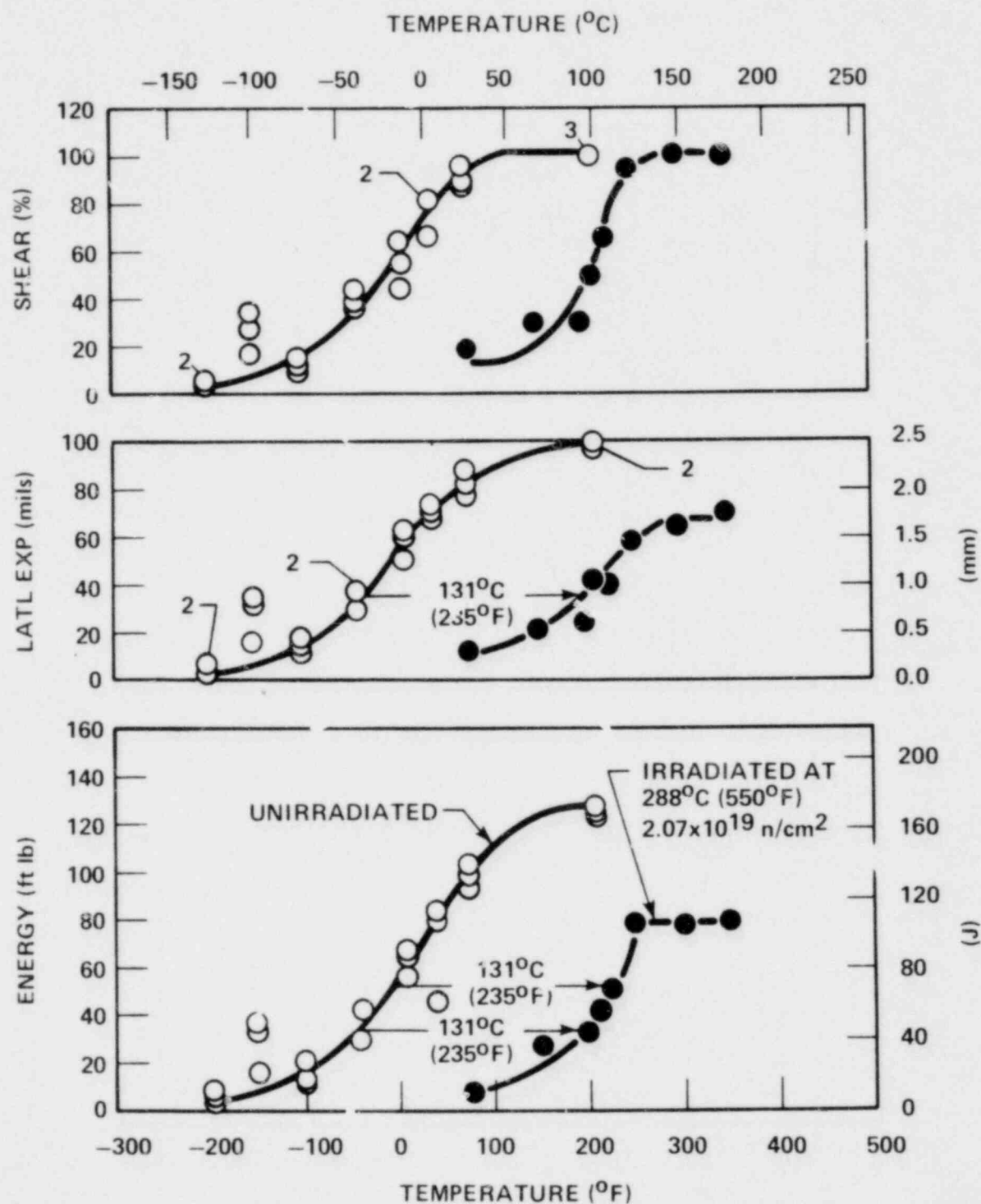


Figure 5-3. Charpy V-Notch Impact Data for Kewaunee Reactor Vessel Weld Metal

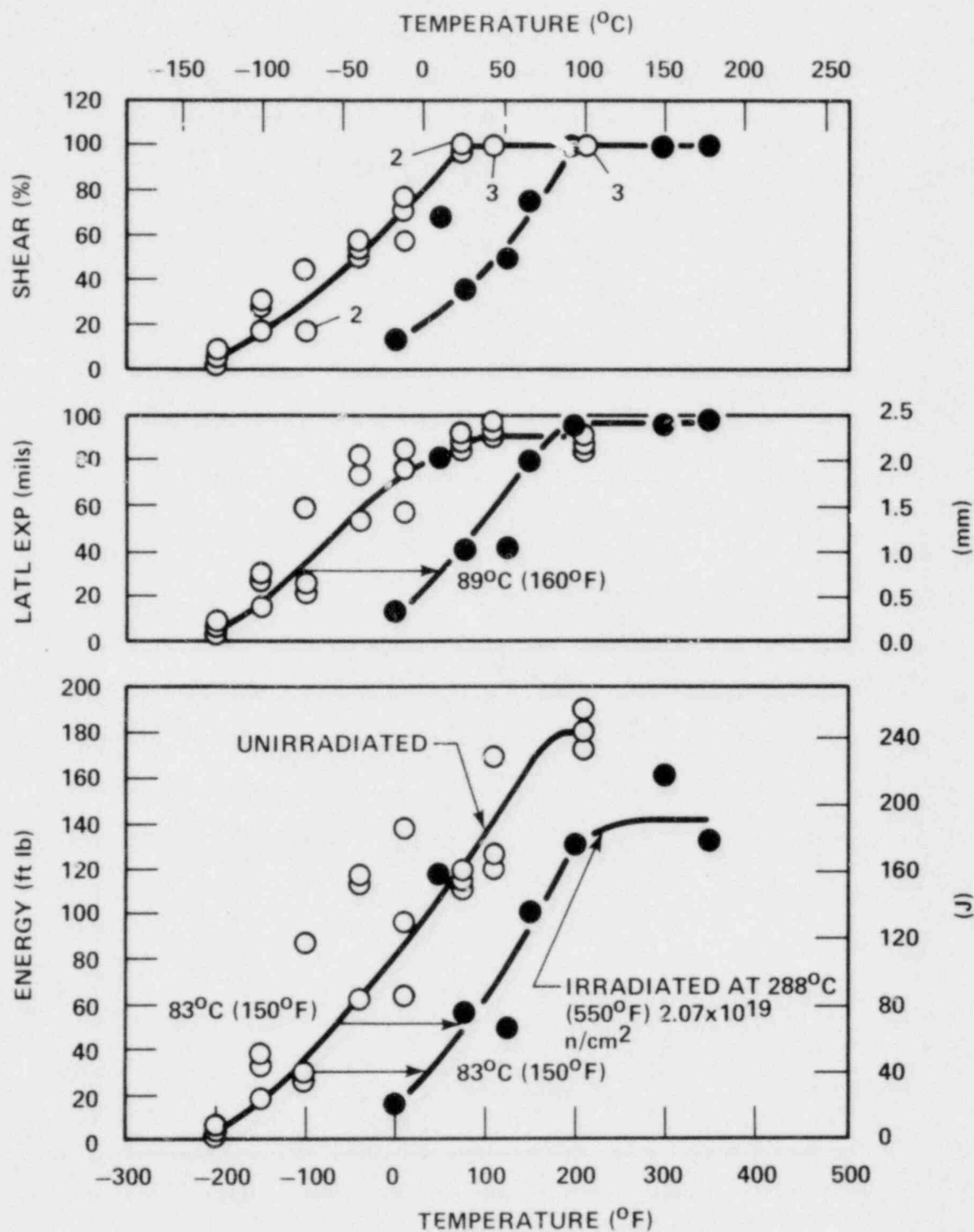


Figure 5-4. Charpy V-Notch Impact Data for Kewaunee Reactor Vessel Weld HAZ Metal

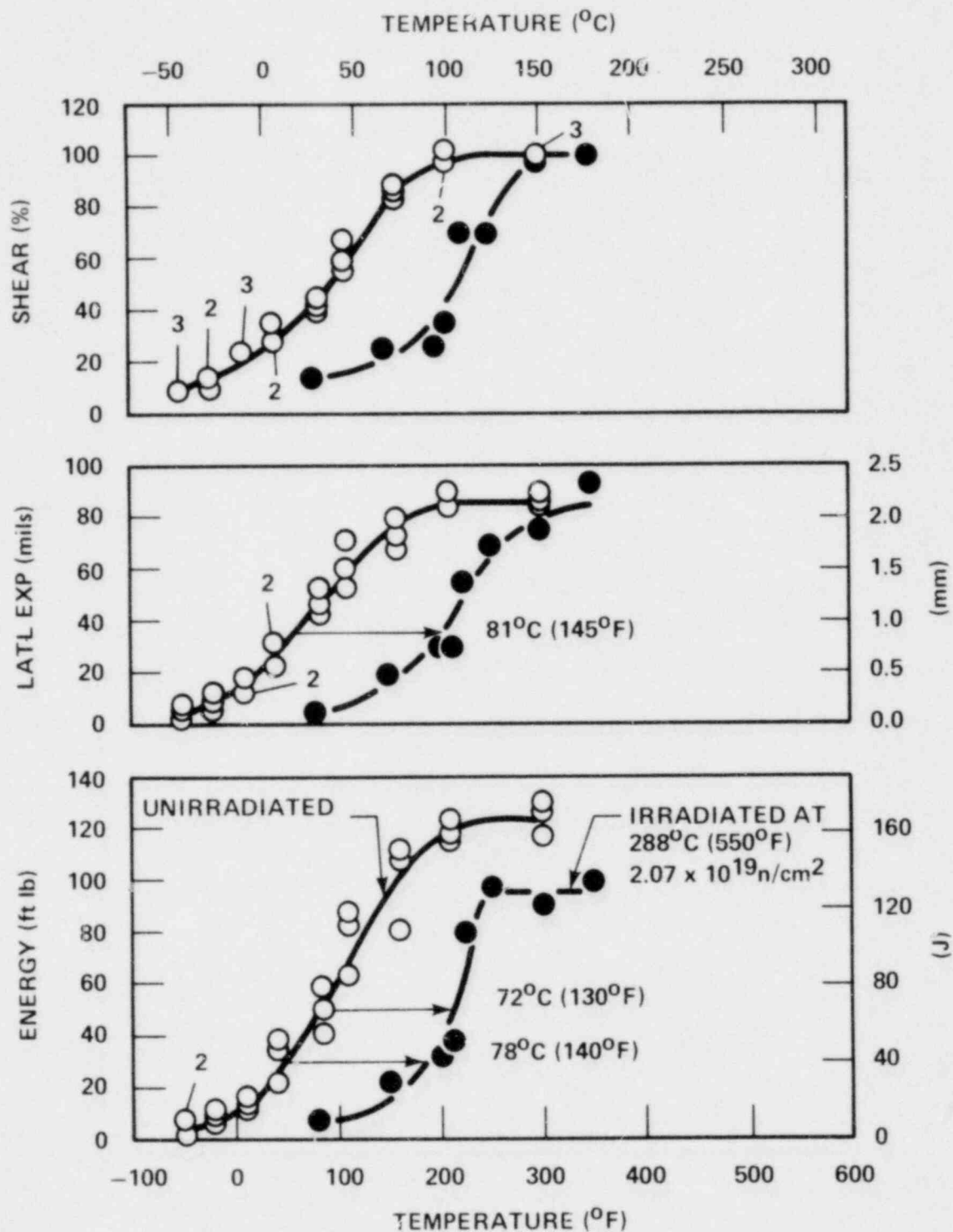


Figure 5-5. Charpy V-Notch Impact Data for A533 Grade B Class 1 ASTM Correlation Monitor Material

Sample Number	Test Temp (°C)	Charpy Energy (J)	Normalized En	
			Charpy Ed/A (kJ/m ²)	Init Em/A (kJ/m ²)
P23	-46	11.0	136	68
P16	-32	17.5	220	101
P18	-18	59.0	737	675
P21	-18	97.5	1220	651
P13	-1	151.0	1890	737
P14	26	68.5	856	628
P17	26	170.0	2127	768
P24	52	164.5	2059	783
P15	93	170.0	2127	698
P20	121	228.0	2847	698
P22	149	210.0	2627	651
S20	-73	9.5	119	84
S13	-46	44.5	559	470
S19	-32	74.0	924	667
S21	-32	77.5	966	683
S15	-18	35.5	441	
S23	-18	77.5	966	698
S22	-1	131.5	1644	714
S24	10	103.5	1297	760
S14	16	135.5	1695	698
S18	26	221.0	2762	729
S16	66	198.5	2483	698
S17	93	203.5	2542	651

TABLE 5-4

DOCUMENTED CHARPY IMPACT TEST RESULTS FOR KEWAUNEE
SHELL FORGINGS

Prop Ep/A (kJ/m ²)	Yield Load (N)	Time to Yield (μ s)	Maximum Load (N)	Time to Maximum (μ s)	Fracture Load (N)	Arrest Load (N)	Yield Stress (MPa)	Flow Stress (MPa)
Forging 122X208VA1								
68			17300	130	17300	0		
119	14900	90	16700	200	16700	0	767	812
62	15100	100	19300	670	19300	0	778	887
569	14900	110	19100	680	17800	0	767	875
1153	14900	130	19600	730	14900	4400	767	887
228	12900	115	18700	690	18700	3300	664	812
1359	13600	140	18000	800	11100	3300	698	812
1276	13300	140	18700	850	12900	6000	687	824
1429	13100	115	18200	790	10900	6400	675	807
2149	12200	130	17600	840			629	767
1975	10700	90	16500	800			549	698
Forging 123X167VA1								
34			17800	90	17800	0		
90	16000	130	19800	500	19800	0	824	921
257	15600	100	20200	660	19800	0	801	921
283	14900	130	20200	670	19600	0	767	904
268	15300	110	19800	670	19600	0	790	904
930	14900	130	19300	700	15300	0	767	881
537	14700	110	20000	730	18900	0	755	893
997	14000	110	19100	700	13800	0	721	853
2033	14500	120	20000	750			744	887
1785	12900	120	19100	730			664	824
1891	12900	130	17300	807			664	778

INSTRUMENT

Sample Number	Test Temp (°C)	Charpy Energy (J)	Normalized Energies		
			Charpy Ed/A (kJ/m ²)	Init Em/A (kJ/m ²)	
W10	26	10.0	127	68	
W15	66	36.0	449	381	
W11	93	42.5	534	365	
W16	99	55.0	686	462	
W12	107	67.0	839	397	
W9	121	106.5	1330	486	
W14	149	105.0	1313	429	
W13	177	107.0	1339	502	
H10	-18	21.0	263	198	
H13	10	159.5	1991	737	
H14	26	75.0	941	557	
H11	52	67.0	839	565	
H9	66	137.0	1712	659	
H16	93	177.0	2212	745	
H12	149	218.5	2729	659	
H15	177	179.5	2246	644	

TABLE 5-5

ED CHARPY IMPACT TEST RESULTS FOR KEWAUNEE WELD METAL
AND HAZ MATERIAL

Temp (°F/A °C/m ²)	Yield Load (N)	Time to Yield (μs)	Maximum Load (N)	Time to Maximum (μs)	Fracture Load (N)	Arrest Load (N)	Yield Stress (MPa)	Flow Stress (MPa)
Weld Metal								
60			16000	90	16000	0		
68	14200	120	18000	400	18000	6200	732	830
169	15100	110	18200	410	18200	7600	778	858
225	14700	100	18500	480	18500	10700	755	853
442	14700	110	18900	430	18900	14200	755	864
845	13300	140	18200	550			687	812
884	12900	130	17600	510			664	784
837	13800	130	17800	530			709	812
HAZ Material								
65	14500	117	17600	265	17600	0	744	824
255	13800	100	19800	730	14500	10200	709	864
384	13800	120	20500	640	20000	6200	709	881
274	15600	130	18900	610	17800	6700	801	887
052	14200	130	18700	730	13800	11100	732	847
467	15100	112	20000	780			778	904
069	12900	150	17300	780			664	778
602	13100	180	17100	760			675	778

Sample Number	Test Temp (°C)	Charpy Energy (J)	Normalized	
			Charpy Ed/A (kJ/m ²)	Init Em/ (kJ/m ²)
R13	26	10.0	127	84
R12	66	30.5	381	316
R9	93	44.0	551	373
R10	99	50.0	627	494
R16	107	109.0	1364	620
R15	121	131.5	1644	698
R11	149	122.5	1534	581
R14	177	134.0	1678	589

TABLE 5-6

INSTRUMENTED CHARPY IMPACT TEST RESULTS FOR THE ASTM
CORRELATION MONITOR MATERIAL

Energies		Yield Load (N)	Time to Yield (μ s)	Maximum Load (N)	Time to Maximum (μ s)	Fracture Load (N)	Arrest Load (N)	Yield Stress (MPa)	Flow Stress (MPa)
2)	Prop Ep/A (kJ/m ²)								
	43			14200	90	14200	0		
	65	14700	130	16900	340	16900	3300	755	812
	178	14000	110	18200	440	17800	6000	721	830
	134	13300	120	18700	540	18700	8900	687	824
	744	13600	130	18200	640	17300	16200	698	818
	946	13800	130	19600	807	16900	11100	709	858
	953	13300	150	18200	660			687	812
	1089	12900	115	17800	630			664	790

THE EFFECT OF
NOTCH TOUGHNESS PRO

Material	Transition Tempera			
	Unirradiated			
	50 ft lb 68 J °C (°F)	30 ft lb 41 J °C (°F)	35 mils .9 mm °C (°F)	50 ft lb 68 J °C (°F)
122X208VA1	-9 (15)	-31 (-25)	-9 (-15)	-9 (25)
123X167VA1	-31 (-25)	-46 (-50)	-43 (-45)	-20 (-5)
Weld Metal	-23 (-10)	-46 (-50)	-37 (-35)	10 (22)
HAZ Metal (122X208VA1)	-57 (-70)	-82 (-115)	-73 (-100)	27 (80)
Correlation	27 (80)	7 (45)	16 (60)	9 (21)

TABLE 5-7

288°C IRRADIATION TO 2.07×10^{19} n/cm² (E > 1 Mev) ON THE
 PROPERTIES OF KEWAUNEE REACTOR VESSEL SURVEILLANCE TEST MATERIAL

Temperature			Δ Transition Temperature			Average Energy Absorption		
Irradiated						at Full Shear		
50 ft lb	30 ft lb	35 mils	50 ft lb	30 ft lb	35 mils	Unirradiated	Irradiated	Δ Energy
68 J	41 J	.9 mm	68 J	41 J	.9 mm	J (ft lb)	J (ft lb)	J (ft lb)
(°C (°F))	(°C (°F))	(°C (°F))	(°C (°F))	(°C (°F))	(°C (°F))			
8	-23	-18	6	8	8	217	217	0
5	(-10)	(0)	(10)	(15)	(15)	(160)	(160)	(0)
0	-34	-26	11	11	17	213	207	6
5	(-30)	(-15)	(20)	(20)	(30)	(157)	(153)	(4)
7	85	93	131	131	131	171	106	65
5	(185)	(200)	(235)	(235)	(235)	(126)	(78)	(48)
7	2	16	83	83	89	244	191	53
0	(35)	(60)	(150)	(150)	(160)	(180)	(141)	(39)
9	85	96	72	78	81	167	129	38
0	(185)	(205)	(130)	(140)	(145)	(123)	(95)	(28)

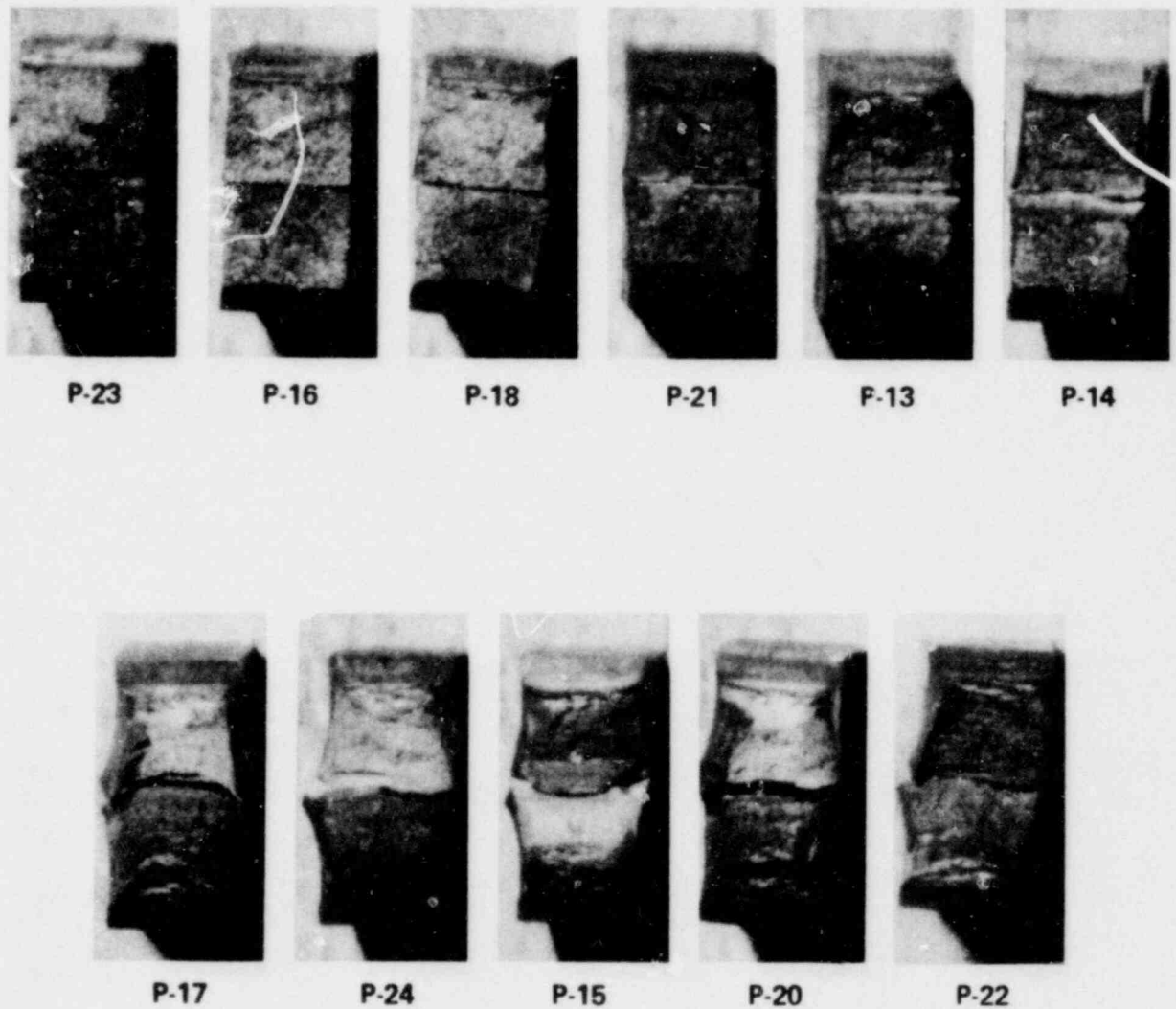


Figure 5-6. Charpy Impact Specimen Fracture Surfaces for Kewaunee Intermediate Shell Forging 122x208 VA1

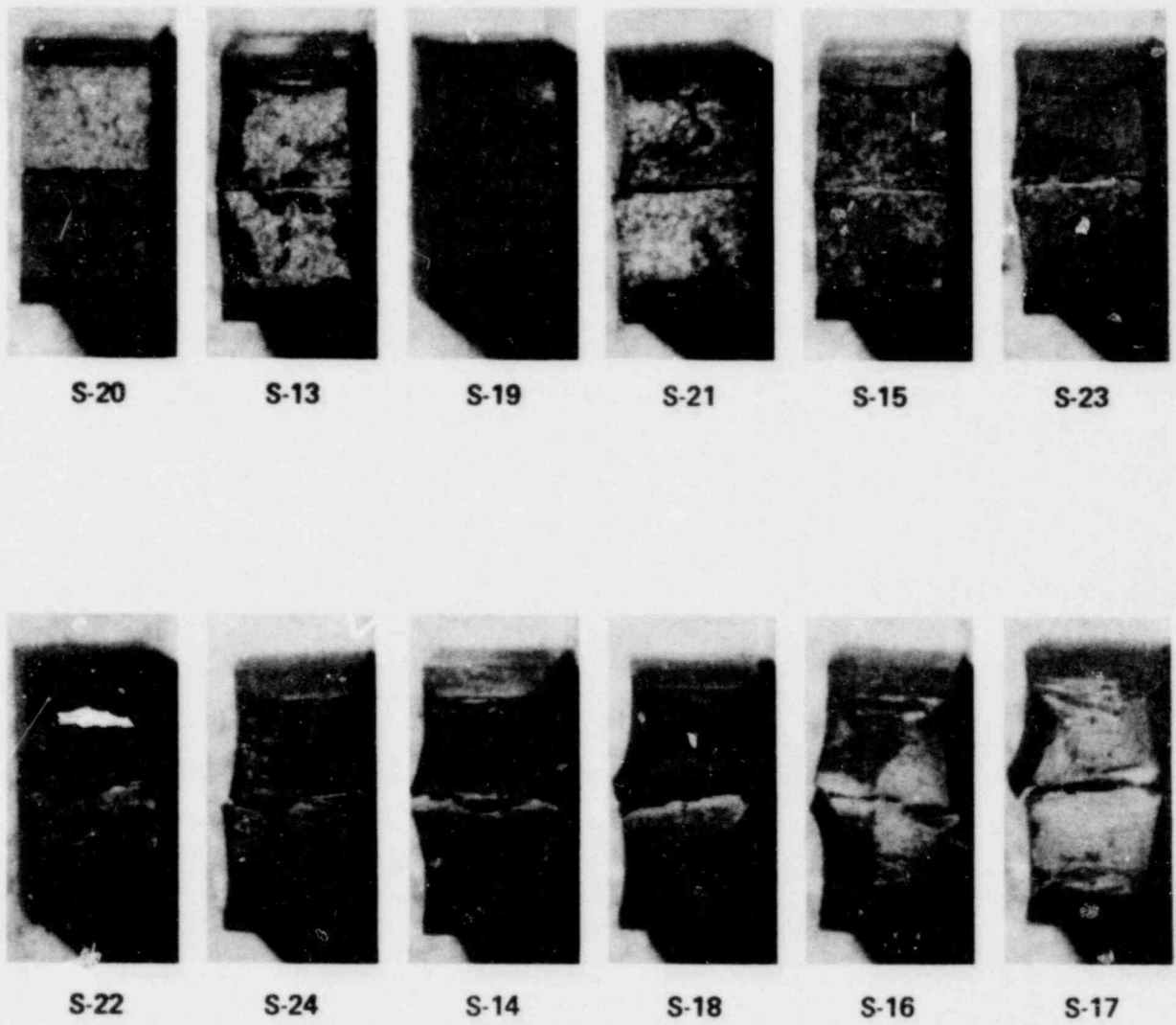


Figure 5-7. Charpy Impact Specimen Fracture Surfaces for Kewaunee Lower Shell Forging 123x167 VA1

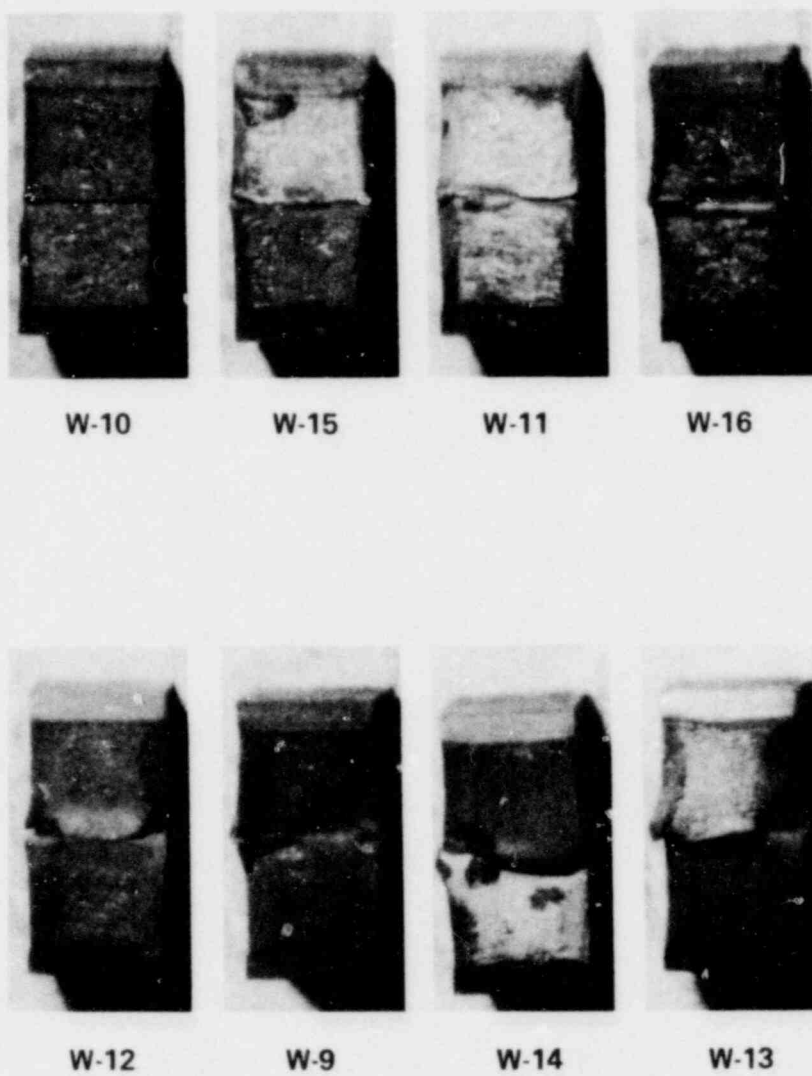


Figure 5-8. Charpy Impact Specimen Fracture Surfaces for Kewaunee Weld Metal

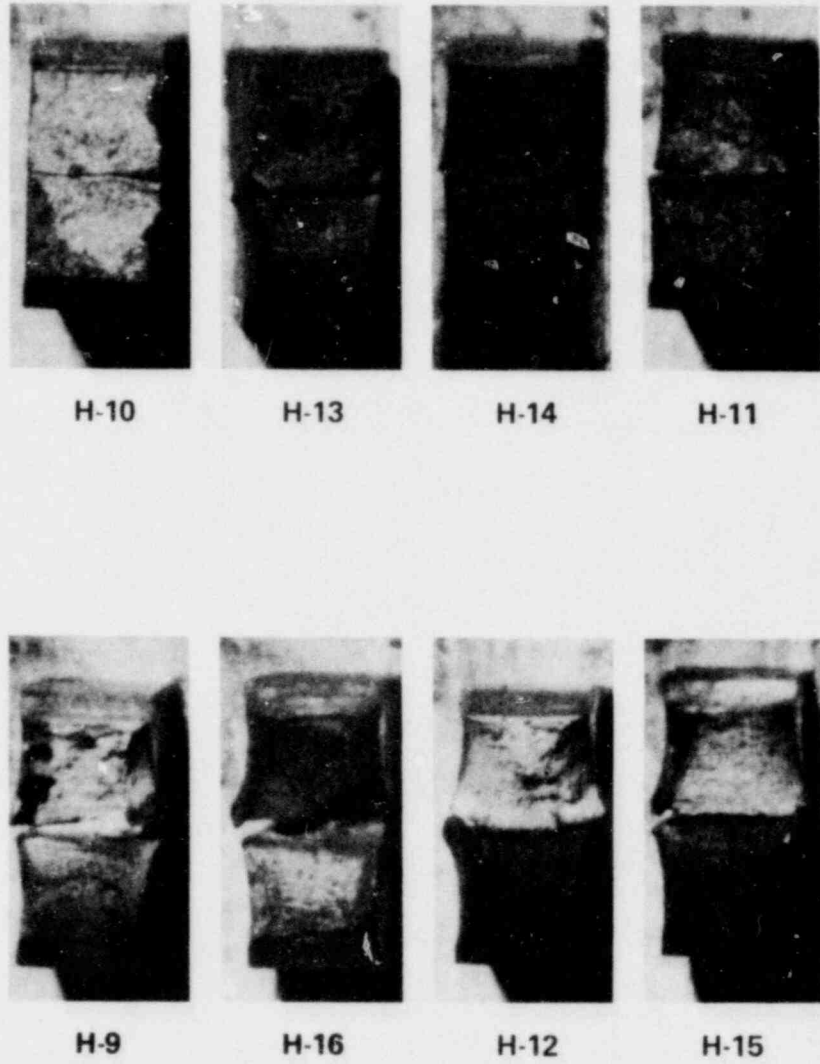


Figure 5-9. Charpy Impact Specimen Fracture Surfaces for Kewaunee HAZ Material

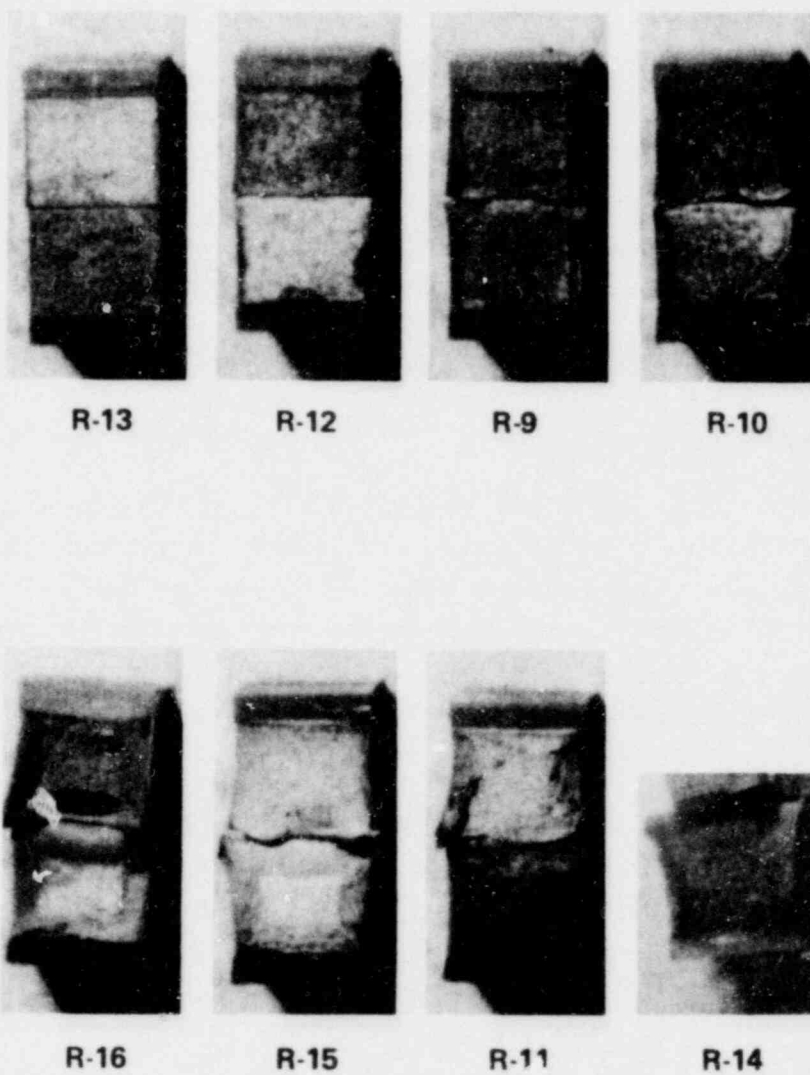


Figure 5-10. Charpy Impact Specimen Fracture Surfaces for Kewaunee ASTM Correlation Monitor Material

Irradiation of material from intermediate shell forging 122X208VA1 to 2.07×10^{19} n/cm² resulted in 68-joule (50 ft lb) and 41-joule (30 ft lb) transition temperature increases of 6°C (10°F) and 8°C (15°F), respectively, as noted in figure 5-1. As shown in figure 5-2, the 68-joule and 41-joule transition temperature increase for material from lower shell forging 123X167VA1 was 11°C (20°F). No decrease in upper shelf energy appears to have occurred for forging 122X208VA1 and only a 6-joule (4 ft lb) decrease was exhibited by forging 123X167VA1.

Irradiation to 2.07×10^{19} n/cm² resulted in a 68-joule and 41-joule transition temperature increase of 131°C (235°F) for the weld metal (figure 5-3). The upper shelf energy of the weld metal decreased by 65 joules (48 ft lb) to 106 joules (78 ft lb) which is sufficiently high enough to allow for continued safe operation of the plant. Weld HAZ material shown in figure 5-4 exhibited a 68-joule and 41-joule transition temperature increase of 83°C (150°F) after irradiation to 2.07×10^{19} n/cm² and a decrease in upper shelf energy of 53 joules (39 ft lb).

ASTM correlation monitor material from HSST Plate 02 exhibited a 68-joule transition temperature increase of 72°C (130°F) and a 41-joule temperature increase of 78°C (140°F) as shown in figure 5-5. Upper shelf energy of the correlation monitor material decreased by 38 joules (28 ft lb).

A summary of the Charpy impact tests performed on the two capsules removed from the Kewaunee reactor to date is shown in table 5-8. These results show that the two low copper (0.06 percent Cu) shell forgings are very insensitive to irradiation up to 2.07×10^{19} n/cm². A comparison of the 41-joule transition temperature increases with the predicted increases based on the U.S. Nuclear Regulatory Commission Regulatory Guide 1.99 Revision 1^[4] is shown in figure 5-10. This comparison shows that the Guide overpredicts the 41-joule transition temperature increase for the forgings by approximately 28°C (50°F).

The results of Charpy impact tests performed to date on the weld metal (0.20 percent Cu) indicate, as shown in table 5-8, that irradiation to 2.07×10^{19} n/cm² resulted in considerable additional increase in transition temperatures when compared with irradiation tests at 5.99×10^{18} n/cm². A comparison of the 41-joule transition temperature increases with the Guide predictions, as shown in figure 5-11, tends to indicate that the Guide will overpredict the transition temperature increase at fluences greater than 2×10^{19} n/cm².

5-3. TENSILE TEST RESULTS

The results of tensile tests performed on material from shell forgings 122X208VA1 and 123X167VA1 and the weld metal are shown in table 5-9 and figures 5-12 through 5-14, respectively. These results show that the 0.2 percent yield strength and other properties of the two forgings are only slightly affected by irradiation to 2.07×10^{19} n/cm². The large increase in 0.2 percent yield strength exhibited by the weld metal as shown in figure 5-14 indicates, as did the Charpy impact tests, that the weld metal is very sensitive to radiation at 2.07×10^{19} n/cm². A typical

TABLE 5-8

**SUMMARY OF KEWAUNEE REACTOR VESSEL SURVEILLANCE CAPSULE
CHARPY IMPACT TEST RESULTS**

Material	Fluence 10^{18} n/cm^2	68 J 50 ft lb Trans. Temp Increase		41 J 30 ft lb Trans. Temp Increase		Decrease in Upper Shelf Energy [a]	
		(°C)	(°F)	(°C)	(°F)	(J)	(ft lb)
Forging 122X208VA1	5.99	0	0	0	0	+27	+20
	20.70	6	10	8	15	0	0
Forging 123X167VA1	5.99	0	0	0	0	+28	+21
	20.70	11	20	11	20	6	4
Weld Metal	5.99	108	195	97	175	60	44
	20.70	131	235	131	235	65	48
Weld HAZ Metal	5.99	44	80	44	80	47.5	35
	20.70	83	150	83	150	53	39
Correlation Monitor	5.99	53	95	53	95	19	14
	20.70	72	130	78	140	38	28

a. Values preceded by a plus sign indicate an increase in upper shelf energy.

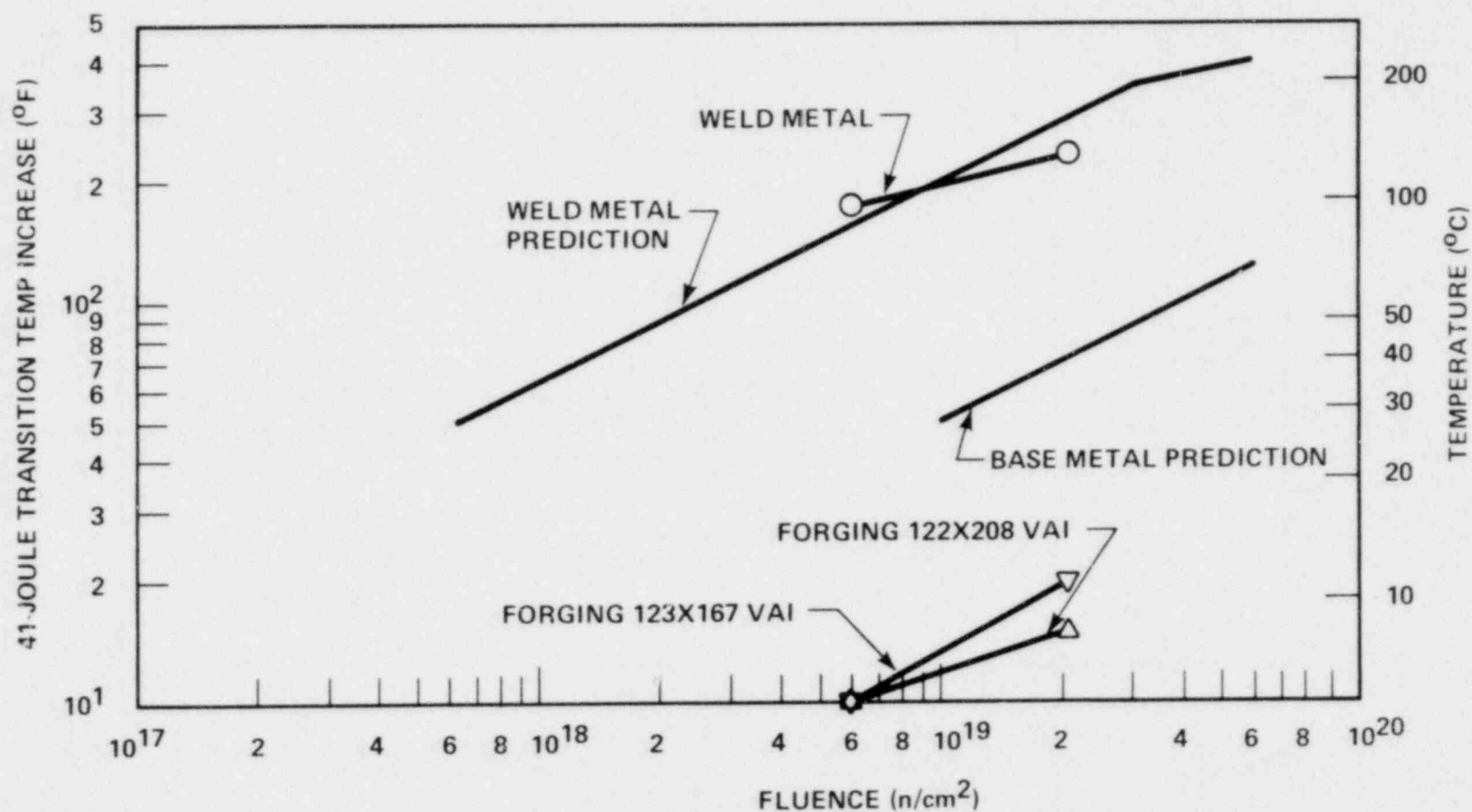


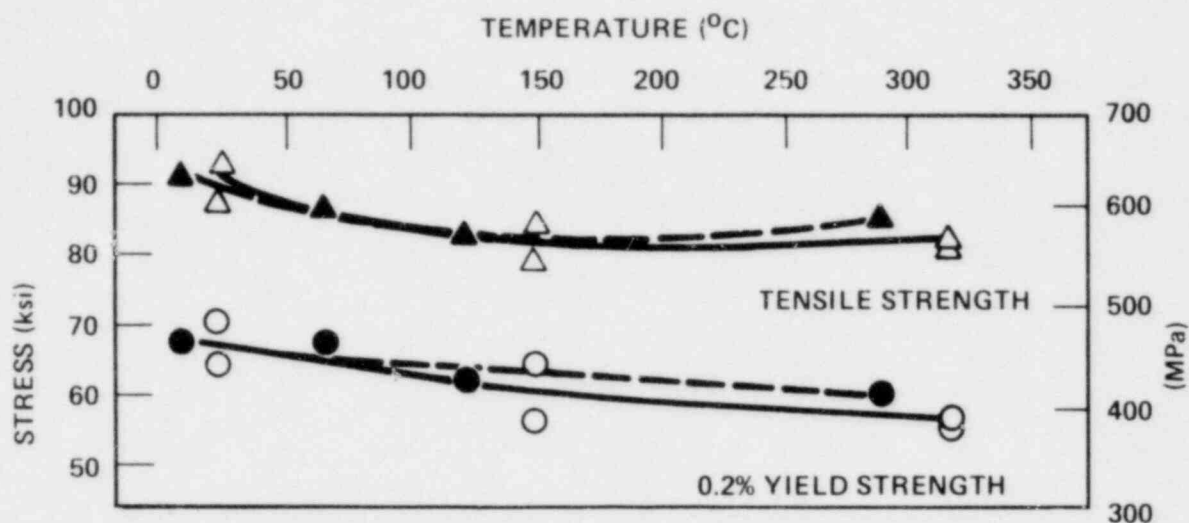
Figure 5-11. Comparison of Predicted Versus Actual 41-Joule Transition Temperature Increases for Kewaunee Reactor Vessel Materials

Sample Number	Material	Test Temp (°C)	.2 S
P-6	122X208VA1	10	
P-5	122X208VA1	66	
P-7	122X208VA1	121	
P-8	122X208VA1	288	
S-6	123X167VA1	-4	
S-5	123X167VA1	24	
S-4	123X167VA1	288	
W-3	Weld	121	
W-4	Weld	288	

TABLE 5-9

TENSILE PROPERTIES FOR KEWAUNEE REACTOR VESSEL MATERIAL
IRRADIATED TO 2.07×10^{19} n/cm² (E > 1 Mev)

% Yield Offset Strength (MPa)	Ultimate Strength (MPa)	Fracture Load (N)	Fracture Stress (MPa)	Fracture Strength (MPa)	Uniform Elongation (%)	Total Elongation (%)	Reduction in Area (%)
467	629	12,700	1480	400	12.0	25.2	73
464	597	11,700	1360	369	11.1	24.8	73
432	572	11,500	1240	362	10.5	22.8	71
414	586	11,800	1190	372	10.7	22.0	69
527	674	12,900	1400	407	11.0	24.9	71
499	646	12,200	1550	386	11.3	24.9	75
435	607	12,000	1210	379	9.8	20.5	69
674	758	16,900	1300	534	12.0	22.5	59
604	716	17,700	1210	558	12.0	19.2	54



LEGEND:
 OPEN POINTS - UNIRRADIATED
 CLOSED POINTS - IRRADIATED AT $2.07 \times 10^{19} \text{ n/cm}^2$

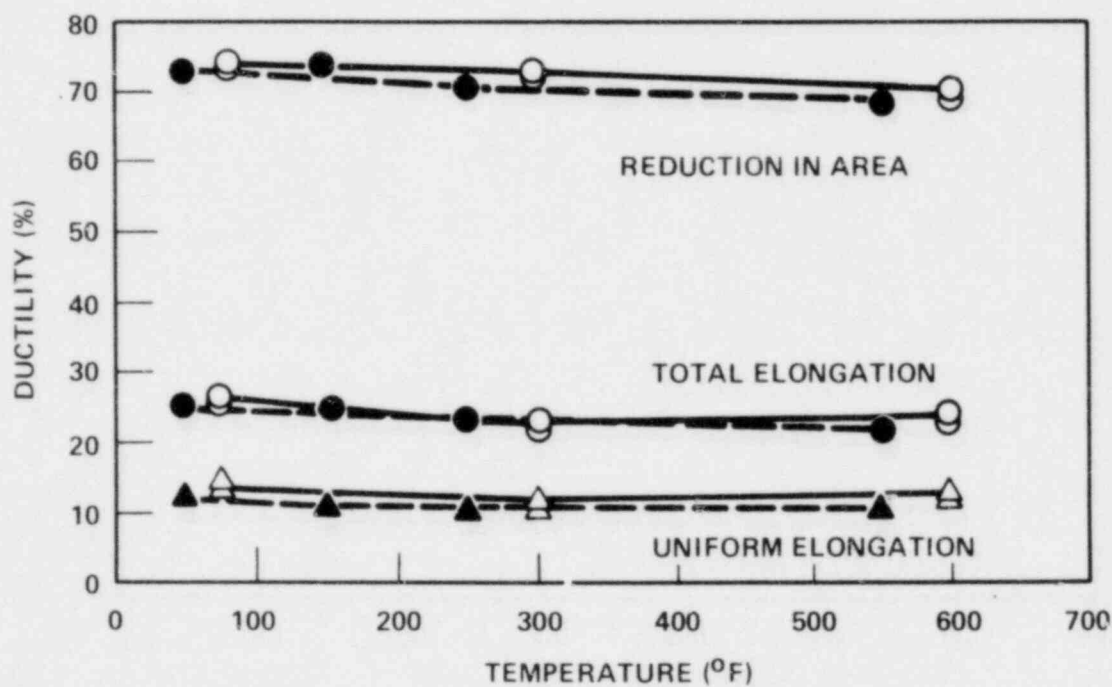
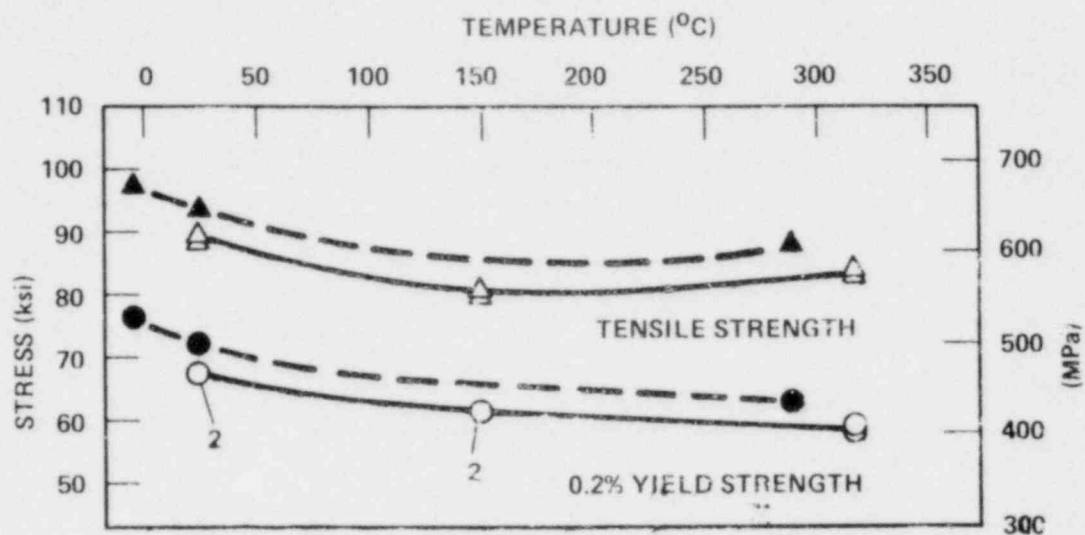


Figure 5-12. Tensile Properties for Kewaunee Reactor Vessel Shell Forging 122x208 VA1



LEGEND:

OPEN POINTS – UNIRRADIATED

CLOSED POINTS – IRRADIATED AT $2.07 \times 10^{19} \text{ n/cm}^2$

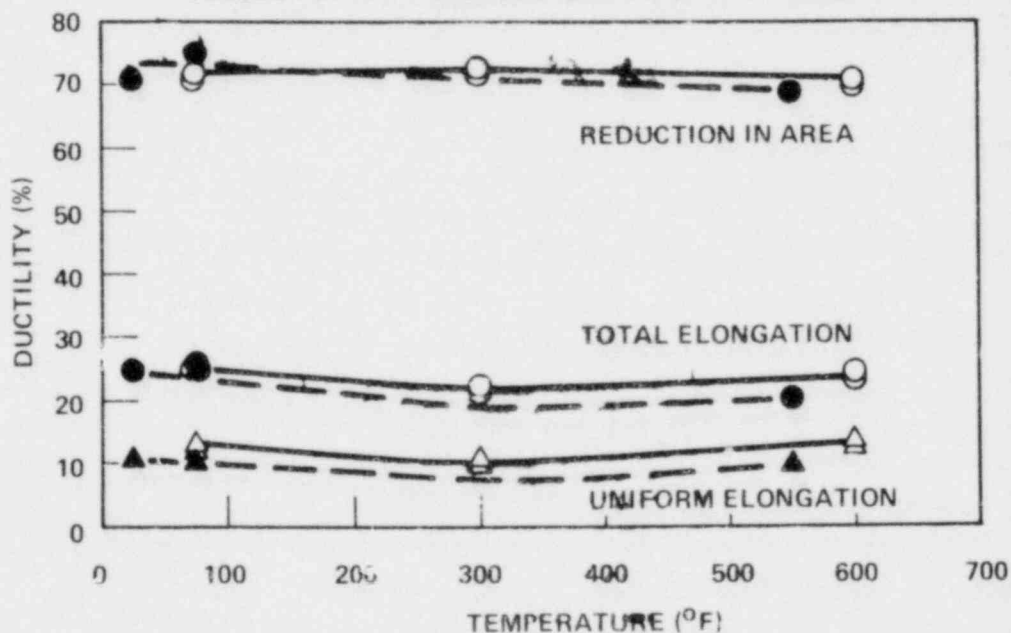
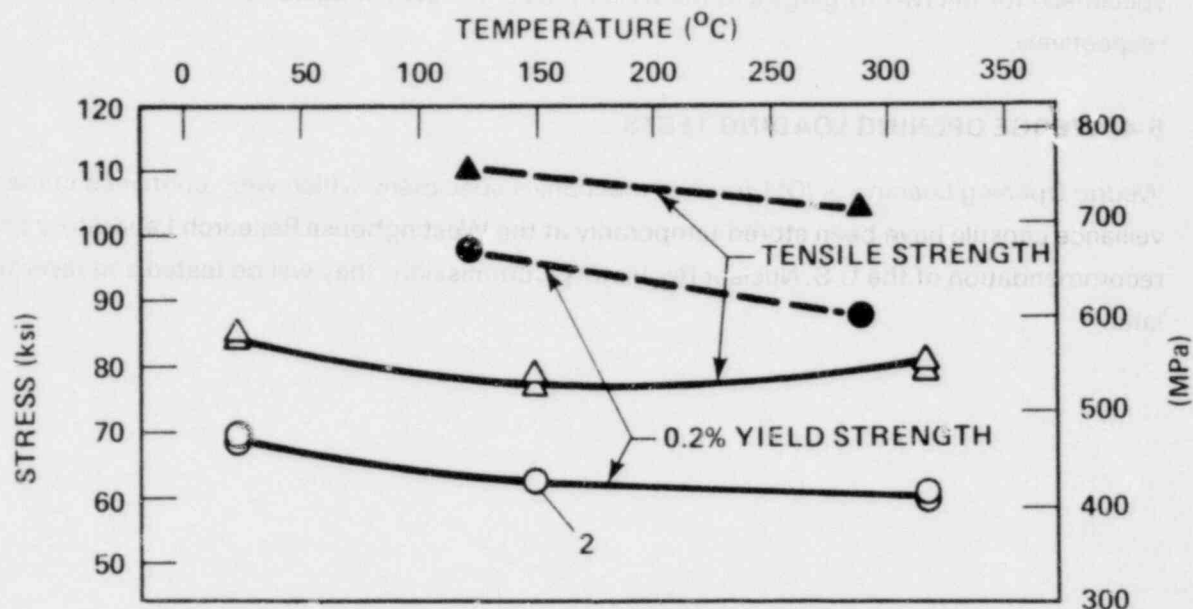


Figure 5-13. Tensile Properties for Kewaunee Reactor Vessel Shell Forging 123x167 VA1



LEGEND:

OPEN POINTS - UNIRRADIATED

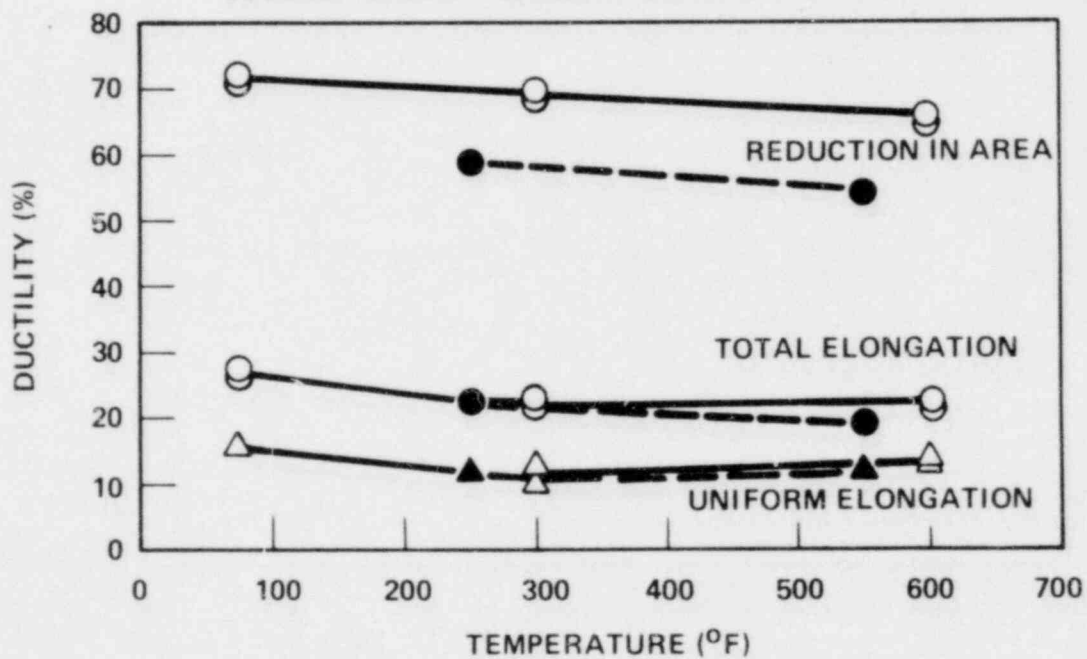
CLOSED POINTS - IRRADIATED AT $2.07 \times 10^{19} \text{ n/cm}^2$ 

Figure 5-14. Tensile Properties for Kewaunee Reactor Vessel Weld Metal

stress strain curve for the tensile tests is shown in figure 5-15. Photographs of the fractured tensile specimens for the two forgings and the weld metal are shown in figures 5-16 through 5-18, respectively.

5-4. WEDGE OPENING LOADING TESTS

Wedge Opening Loading (WOL) fracture mechanics specimens which were contained in the surveillance capsule have been stored temporarily at the Westinghouse Research Laboratory on the recommendation of the U.S. Nuclear Regulatory Commission; they will be tested and reported on later.

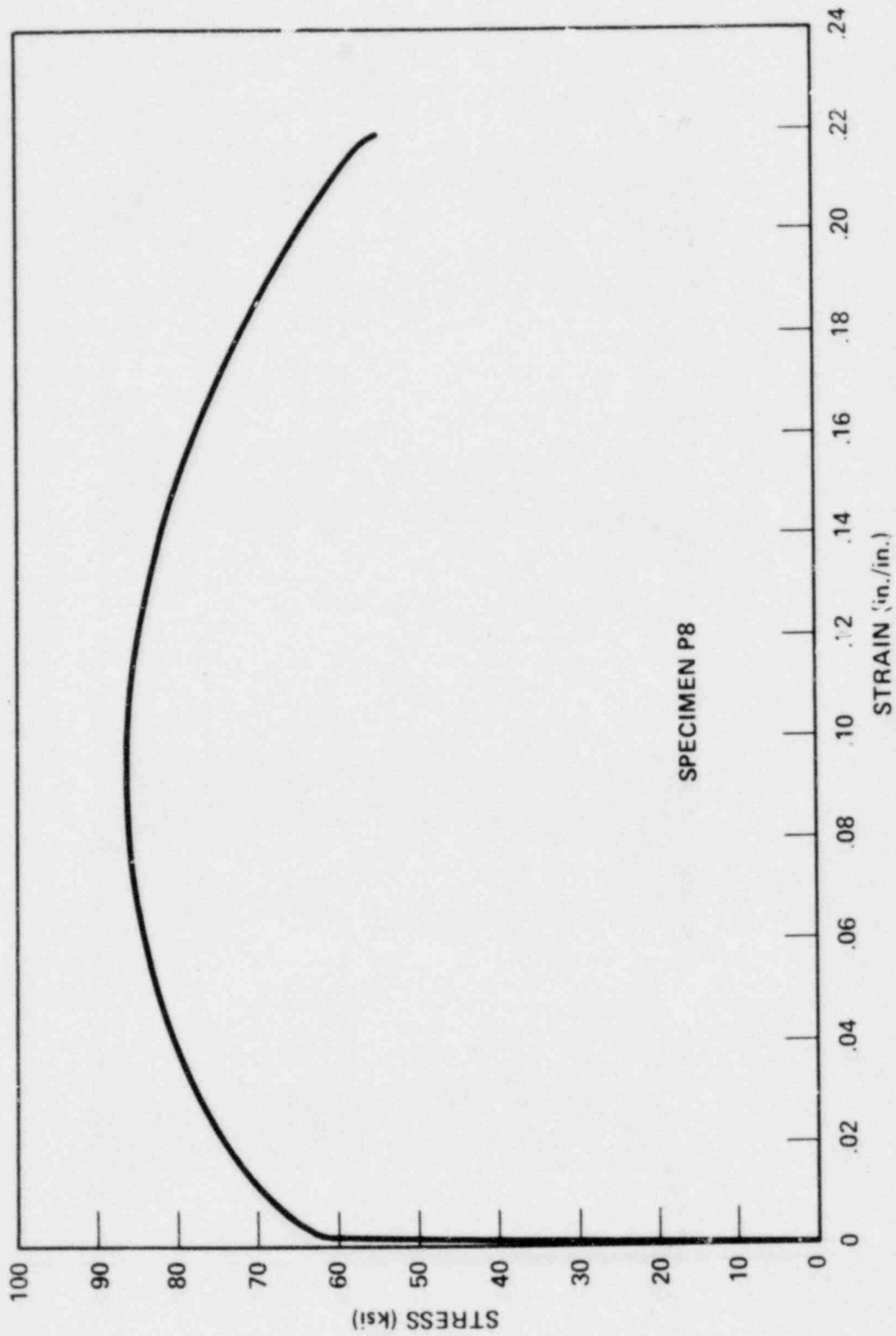
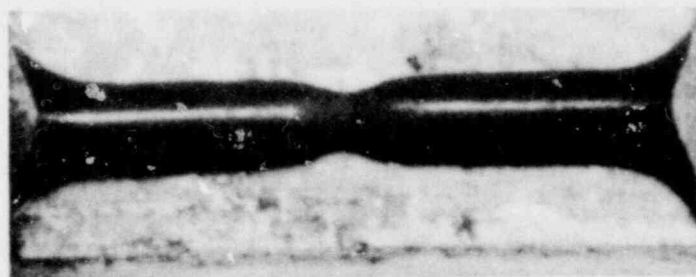
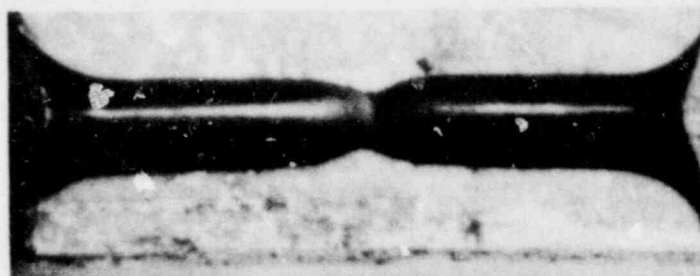


Figure 5-15. Typical Stress-Strain Curve for Tension Specimens



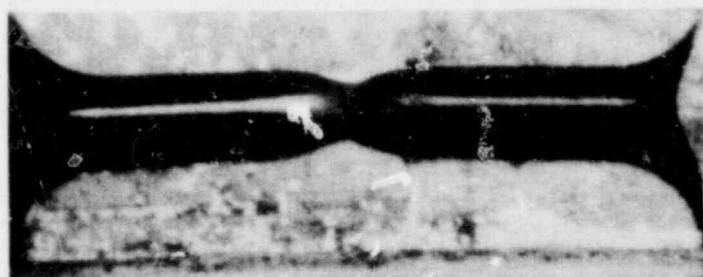
P-6

10 C



P-5

66 C



P-7

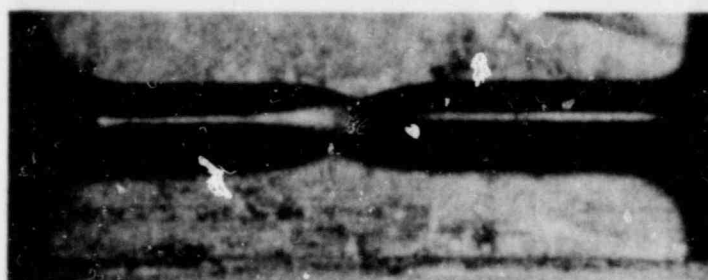
121 C



P-8

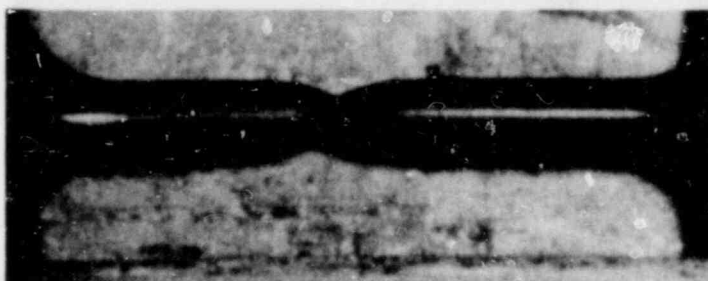
288 C

Figure 5-16. Fractured Tensile Specimens From Kewaunee Intermediate Shell Forging 122x208 VA1



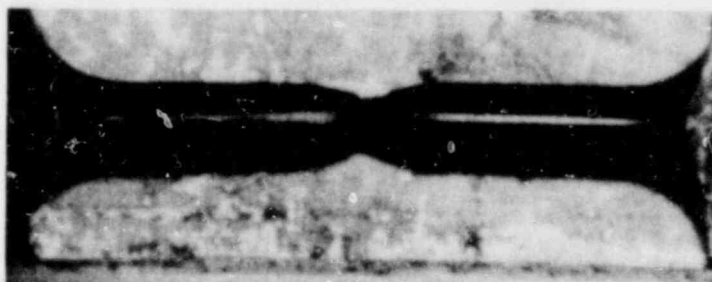
S-6

-4 C



S-5

24 C



S-4

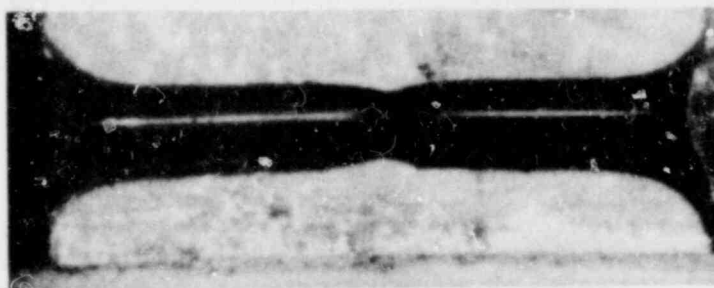
288 C

Figure 5-17. Fractured Tensile Specimens From Kewaunee Lower Shell Forging 123x167 VA1



W-3

121 C



W-4

288 C

Figure 5-18. Fractured Tensile Specimens From Kewaunee Weld Metal

SECTION 6

RADIATION ANALYSIS AND NEUTRON DOSIMETRY

6-1. INTRODUCTION

Knowledge of the neutron environment within the pressure vessel-surveillance capsule geometry is required as an integral part of LWR pressure vessel surveillance programs for two reasons. First, in the interpretation of radiation-induced property changes observed in materials test specimens, the neutron environment (fluence, flux) to which the test specimens were exposed must be known. Second, in relating the changes observed in the test specimens to the present and future condition of the reactor vessel, a relationship between the environment at various positions within the reactor vessel and that experienced by the test specimens must be established. The former requirement is normally met by employing a combination of rigorous analytical techniques and measurements obtained with passive neutron flux monitors contained in each of the surveillance capsules. The latter requirement is derived solely from analysis.

This section describes a discrete ordinates S_n transport analysis performed for the Kewaunee reactor to determine the fast neutron ($E > 1.0$ Mev) flux and fluence as well as the neutron energy spectra within the reactor vessel and surveillance capsules, and, in turn, to develop lead factors for use in relating neutron exposure of the pressure vessel to that of the surveillance capsules. Based on spectrum-averaged reaction cross sections derived from this calculation, the analysis of the neutron dosimetry contained in Capsule R is discussed, and updated evaluations of dosimetry from Capsule V are presented.

6-2. DISCRETE ORDINATES ANALYSIS

A plan view of the Kewaunee reactor geometry at the core midplane is shown in figure 6-1. Because the reactor exhibits 1/8th core symmetry, only a zero- to 45-degree sector is depicted. Six irradiation capsules attached to the thermal shield are included in the design to constitute the reactor vessel surveillance program. Two capsules are located symmetrically at 13, 23, and 33 degrees from the cardinal axis as shown in figure 6-1.

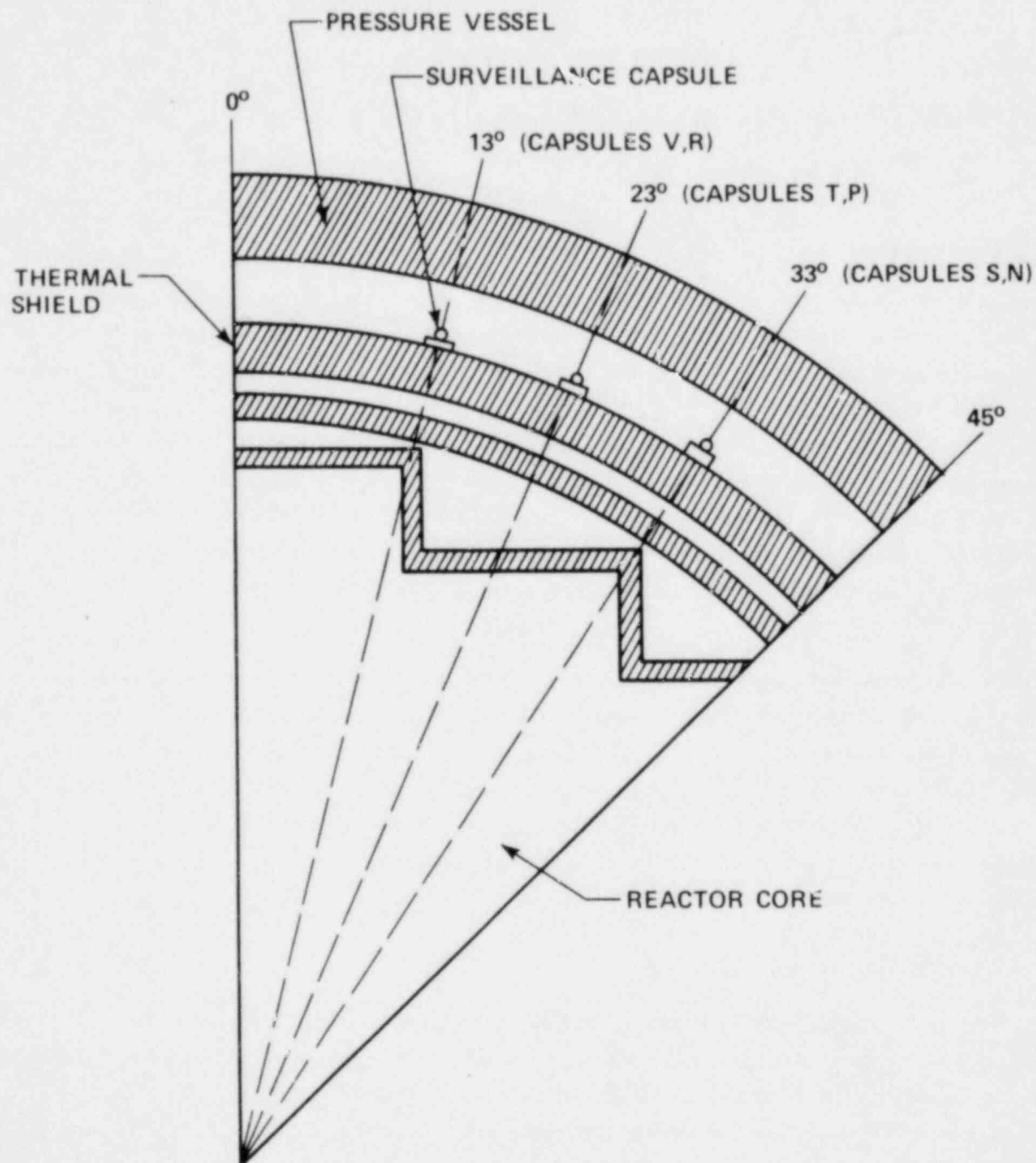


Figure 6-1. Kewaunee Reactor Geometry

A plan view of a single surveillance capsule attached to the thermal shield is shown in figure 6-2. The stainless steel specimen container is 1-inch square and approximately 63 inches in height. The containers are positioned axially such that the specimens are centered on the core midplane, thus spanning the central 5.25 feet of the 12-foot-high reactor core.

From a neutronic standpoint, the surveillance capsule structures are significant. In fact, they have a marked impact on the distributions of neutron flux and energy spectra in the water annulus between the thermal shield and the reactor vessel. Thus, to properly ascertain the neutron environment at the test specimen locations, the capsules themselves must be included in the analytical model. Use of at least a two-dimensional computation is, therefore, mandatory.

In the analysis of the neutron environment within the Kewaunee reactor geometry, predictions of neutron flux magnitude and energy spectra were made with the DOT^[5] two-dimensional discrete ordinates code. The radial and azimuthal distributions were obtained from an R,θ computation wherein the geometry shown in figures 6-1 and 6-2 was described in the analytical model. In addition to the R,θ computation, a second calculation in R,Z geometry was also carried out to obtain relative axial variations of neutron flux throughout the geometry of interest. In the R,Z analysis the reactor core was treated as an equivalent volume cylinder and the surveillance capsules were not included in the model.

Both the R,θ and the R,Z analyses employed 21 neutron energy groups, an S_8 angular quadrature, and a P_1 cross-section expansion. The cross sections were generated via the Westinghouse GAMBIT^[6] code system with broad group processing by the APPROPOS^[7] and ANISN^[8] codes. The energy group structure used in the analysis is listed in table 6-1.

A key input parameter in the analysis of the integrated fast neutron exposure of the reactor vessel is the core power distribution. For this analysis, power distributions representative of time-averaged conditions derived from statistical studies of long-term operation of Westinghouse two-loop plants were employed. These input distributions include rod-by-rod spatial variations for all peripheral fuel assemblies.

It should be noted that this particular power distribution is intended to produce accurate end-of-life neutron exposure levels for the pressure vessel. As such, the calculation is indeed representative of an average neutron flux and small (plus or minus 15 to 20 percent) deviations from cycle to cycle are to be expected.

Having the results of the R,θ and R,Z calculations, three-dimensional variations of neutron flux may be approximated by assuming that the following relation holds for the applicable regions of the reactor.

$$\phi(R,Z,\theta,E_g) = \phi(R,\theta,E_g) F(Z,E_g) \quad (6-1)$$

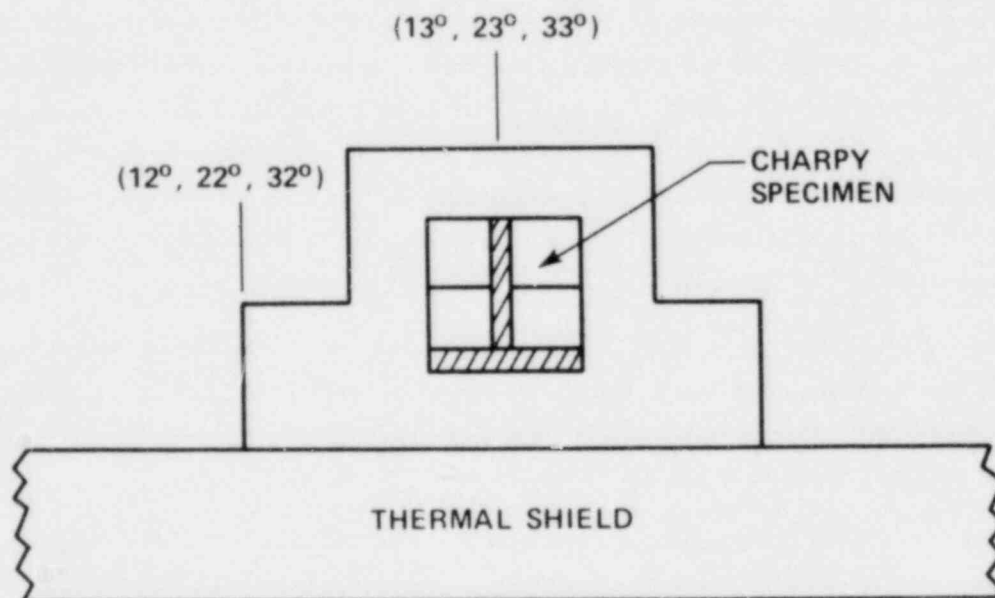


Figure 6-2. Plan View of a Reactor Vessel Surveillance Capsule

TABLE 6-1
21 GROUP ENERGY STRUCTURE

Group	Lower Energy (Mev)
1	7.79[a]
2	6.07
3	4.72
4	3.68
5	2.87
6	2.23
7	1.74
8	1.35
9	1.05
10	0.821
11	0.388
12	0.111
13	4.09×10^{-2}
14	1.50×10^{-2}
15	5.53×10^{-3}
16	5.83×10^{-4}
17	7.89×10^{-5}
18	1.07×10^{-5}
19	1.86×10^{-6}
20	3.00×10^{-7}
21	0.0

a. Upper energy of group 1 is 10.0 Mev

where

$\phi(R,Z,\theta,E_g)$ = neutron flux at point R,Z,θ within energy group g

$\phi(R,\theta,E_g)$ = neutron flux at point R,θ within energy group g obtained from the R,θ calculation

$F(Z,E_g)$ = relative axial distribution of neutron flux within energy group g obtained from the R,Z calculation

6-3. NEUTRON DOSIMETRY

The passive neutron flux monitors included in the Kewaunee surveillance program are listed in table 6-2. The first five reactions in table 6-2 are used as fast neutron monitors to relate neutron fluence ($E > 1.0$ Mev) to measure materials properties changes. To properly account for burnout of the product isotope generated by fast neutron reactions, it is necessary to also determine the magnitude of the thermal neutron flux at the monitor location. Therefore, bare and cadmium-covered cobalt-aluminum monitors were also included.

The relative locations of the various monitors within the surveillance capsules are shown in figure 4-2. The iron, nickel, copper, and cobalt-aluminum monitors, in wire form, are placed in holes drilled in spacers at several axial levels within the capsules. The cadmium-shielded neptunium and uranium fission monitors are accommodated within the dosimeter block located near the center of the capsule.

The use of passive monitors such as those listed in table 6-2 does not yield a direct measure of the energy-dependent flux level at the point of interest. Rather, the activation or fission process is a measure of the integrated effect that the time- and energy-dependent neutron flux has on target material over the course of the irradiation period. An accurate assessment of the average neutron flux level incident on the various monitors may be derived from the activation measurements only if the irradiation parameters are well known. In particular, the following variables are of interest:

- The operating history of the reactor
- The energy response of the monitor
- The neutron energy spectrum at the monitor location
- The physical characteristics of the monitor

The analysis of the passive monitors and subsequent derivation of the average neutron flux requires completion of two procedures. First, the disintegration rate of product isotope per unit mass of monitor must be determined. Second, in order to define a suitable spectrum averaged reaction cross section, the neutron energy spectrum at the monitor location must be calculated.

TABLE 6-2

NUCLEAR PARAMETERS FOR NEUTRON FLUX MONITORS

Monitor Material	Target Reaction of Interest	Weight Fraction	Response Range	Product Half-Life	Fission Yield (%)
Copper	$\text{Cu}^{63}(\text{n}, \alpha)\text{Co}^{60}$	0.6917	$E > 4.7 \text{ Mev}$	5.27 years	6.3 6.5
Iron	$\text{Fe}^{54}(\text{n}, \text{p})\text{Mn}^{54}$	0.0585	$E > 1.0 \text{ Mev}$	314 days	
Nickel	$\text{Ni}^{58}(\text{n}, \text{p})\text{Co}^{68}$	0.6777	$E > 1.0 \text{ Mev}$	71.4 days	
Uranium-238[a]	$\text{U}^{238}(\text{n}, \text{f})\text{Cs}^{137}$	1.0	$E > 0.4 \text{ Mev}$	30.2 years	
Neptunium-237[a]	$\text{Np}^{237}(\text{n}, \text{f})\text{Cs}^{137}$	1.0	$E > 0.08 \text{ Mev}$	30.2 years	
Cobalt-Aluminum[a]	$\text{Co}^{59}(\text{n}, \gamma)\text{Co}^{60}$	0.0015	$0.4 \text{ eV} > 0.015 \text{ Mev}$	5.27 years	
Cobalt-Aluminum	$\text{Co}^{59}(\text{n}, \gamma)\text{Co}^{60}$	0.0015	$E > 0.0015 \text{ Mev}$	5.27 years	

a Denotes that monitor is cadmium shielded

The specific activity of each of the monitors is determined using established ASTM procedures. [9,10,11,12,13] Following sample preparation, the activity of each monitor is determined by means of a lithium-drifted germanium, Ge(Li), gamma spectrometer. The overall standard deviation of the measured data is a function of the precision of sample weighing, the uncertainty in counting, and the acceptable error in detector calibration. For the samples removed from Kewaunee, the overall 2σ deviation in the measured data is determined to be plus or minus 10 percent. The neutron energy spectra are determined analytically using the method described in paragraph 6-1.

Having the measured activity of the monitors and the neutron energy spectra at the locations of interest, the calculation of the neutron flux proceeds as follows.

The reaction product activity in the monitor is expressed as

$$R = \frac{N_0}{A} f_i Y \int_E \sigma(E) \phi(E) \sum_{j=1}^N \frac{P_j}{P_{\max}} (1 - e^{-\lambda t_j}) e^{-\lambda t_d} \quad (6-2)$$

where

R	=	induced product activity
N_0	=	Avogadro's number
A	=	atomic weight of the target isotope
f_i	=	weight fraction of the target isotope in the target material
Y	=	number of product atoms produced per reaction
$\sigma(E)$	=	energy-dependent reaction cross section
$\phi(E)$	=	energy-dependent neutron flux at the monitor location with the reactor at full power
P_j	=	average core power level during irradiation period j
P_{\max}	=	maximum or reference core power level
λ	=	decay constant of the product isotope
t_j	=	length of irradiation period j
t_d	=	decay time following irradiation period j

Because neutron flux distributions are calculated using multigroup transport methods and, further, because the prime interest is in the fast neutron flux above 1.0 Mev, spectrum-averaged reaction cross sections are defined such that the integral term in equation (6-2) is replaced by the following relation.

$$\int_E \sigma(E) \phi(E) dE = \bar{\sigma} \phi(E > 1.0 \text{ Mev})$$

where

$$\bar{\sigma} = \frac{\int_0^{\infty} \sigma(E) \phi(E) dE}{\int_{1.0 \text{ Mev}}^{\infty} \phi(E) dE} = \frac{\sum_{G=1}^N \sigma_g \phi_g}{\sum_{G=G}^N \phi_g \quad 1.0 \text{ Mev}}$$

Thus, equation (6-2) is rewritten

$$R = \frac{N_0}{A} f_i \gamma \bar{\sigma} \phi(E > 1.0 \text{ Mev}) \sum_{j=1}^N \frac{P_j}{P_{\max}} (1 - e^{-\lambda t_j}) e^{-\lambda t_d}$$

or, solving for the neutron flux,

$$\phi(E > 1.0 \text{ Mev}) = \frac{R}{\frac{N_0}{A} f_i \gamma \bar{\sigma} \sum_{j=1}^N \frac{P_j}{P_{\max}} (1 - e^{-\lambda t_j}) e^{-\lambda t_d}} \quad (6-3)$$

The total fluence above 1.0 Mev is then given by

$$\Phi(E > 1.0 \text{ Mev}) = \phi(E > 1.0 \text{ Mev}) \sum_{j=1}^N \frac{P_j}{P_{\max}} t_j \quad (6-4)$$

where

$$\sum_{j=1}^N \frac{P_j}{P_{\max}} t_j = \text{total effective full power seconds of reactor operation up to the time of capsule removal}$$

An assessment of the thermal neutron flux levels within the surveillance capsules is obtained from the bare and cadmium-covered $\text{Co}^{59}(n, \gamma)\text{Co}^{60}$ data by means of cadmium ratios and the use of a 7-barn 2200 m/s cross section. Thus,

$$\phi_{Th} = \frac{R_{bare} \left\{ \begin{matrix} D-1 \\ D \end{matrix} \right\}}{N_o \sum_{j=1}^N \frac{P_j}{P_{max}} \frac{f_i \gamma \sigma}{(1-e^{-\lambda t_j}) e^{-\lambda t_d}}}$$

where D is defined as $R_{bare}/R_{Cd \text{ covered}}$.

6-4. TRANSPORT ANALYSIS RESULTS

Results of the S_n transport calculations for the Kewaunee reactor are summarized in figures 6-3 through 6-7 and in tables 6-3 through 6-5. In figure 6-3, the calculated maximum neutron flux levels at the surveillance capsule center line, pressure vessel inner radius, 1/4 thickness location, and 3/4 thickness location are presented as a function of azimuthal angle. The influence of the surveillance capsules on the fast neutron flux distribution is clearly evident. In figure 6-4, the radial distribution of maximum fast neutron flux ($E > 1.0$ Mev) through the thickness of the reactor pressure vessel is shown. The relative axial variation of neutron flux within the vessel is given in figure 6-5. Absolute axial variations of fast neutron flux may be obtained by multiplying the levels given in figures 6-3 or 6-4 by the appropriate values from figure 6-5.

In figure 6-6 the radial variations of fast neutron flux within each of the surveillance capsules are presented. These data, in conjunction with the maximum vessel flux, are used to develop lead factors for each of the capsules. Here the lead factor is defined as the ratio of the fast neutron flux ($E > 1.0$ Mev) at the dosimeter block location (capsule center) to the maximum fast neutron flux at the pressure vessel inner radius. Updated lead factors for all of the Kewaunee surveillance capsules are listed in table 6-3. The lead factors presented in table 6-3 differ from those previously published in references 1 and 3 because of an improved neutron transport methodology which takes into account neutron flux perturbations introduced by the surveillance capsules and their associated structure. Additional information on this perturbation effect is given in reference 14.

Because the neutron flux monitors contained within the surveillance capsules are not all located at the same radial location, the measured disintegration rates are analytically adjusted for the gradients that exist within the capsules so that flux and fluence levels may be derived on a common basis at a common location. This point of comparison was chosen to be the capsule center. Analytically determined reaction rate gradients for use in the adjustment procedures are shown in figure 6-7 for Capsules V and R. All of the applicable fast neutron reactions are included.

To derive neutron flux and fluence levels from the measured disintegration rates, suitable spectrum-averaged reaction cross sections are required. The neutron energy spectrum calculated to exist at the center of each of the Kewaunee surveillance capsules is given in table 6-4. The associated spectrum-averaged cross sections for each of the five fast neutron reactions are given in table 6-5.

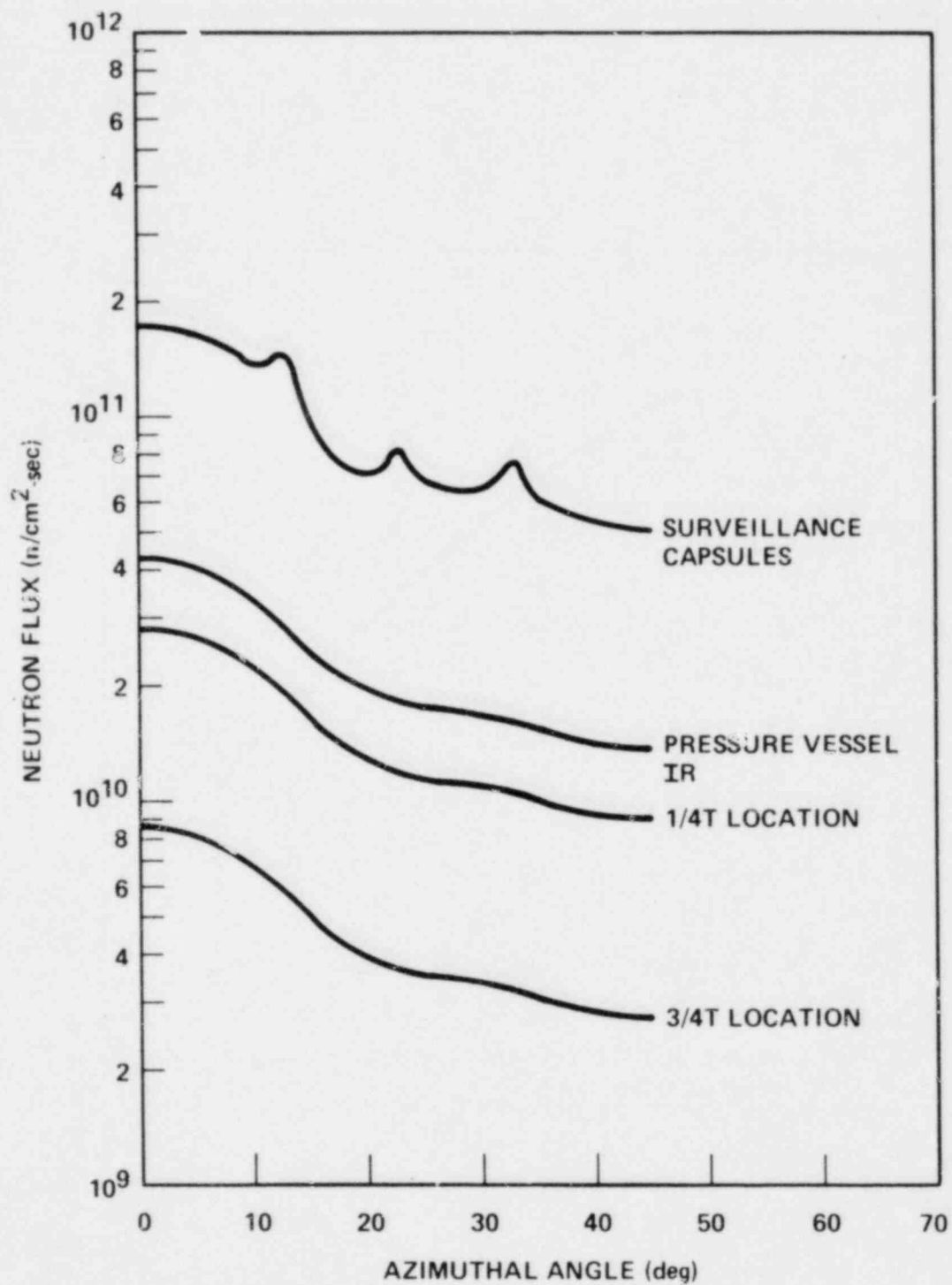


Figure 6-3. Calculated Azimuthal Distribution of Maximum Fast Neutron Flux ($E > 1.0$ Mev) With the Pressure Vessel Surveillance Capsule Geometry

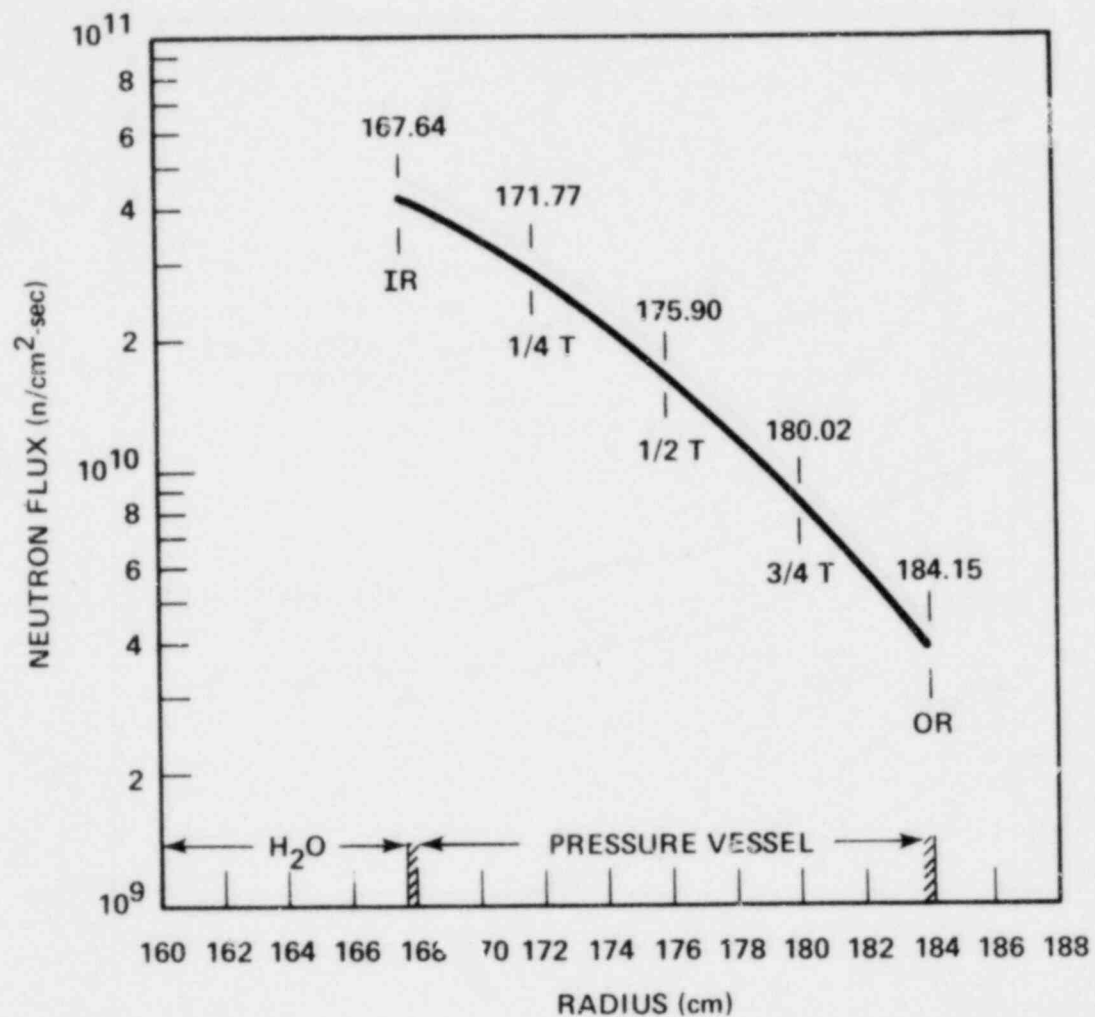


Figure 6-4. Calculated Radial Distribution of Maximum Fast Neutron Flux ($E > 1.0$ Mev) Within the Pressure Vessel

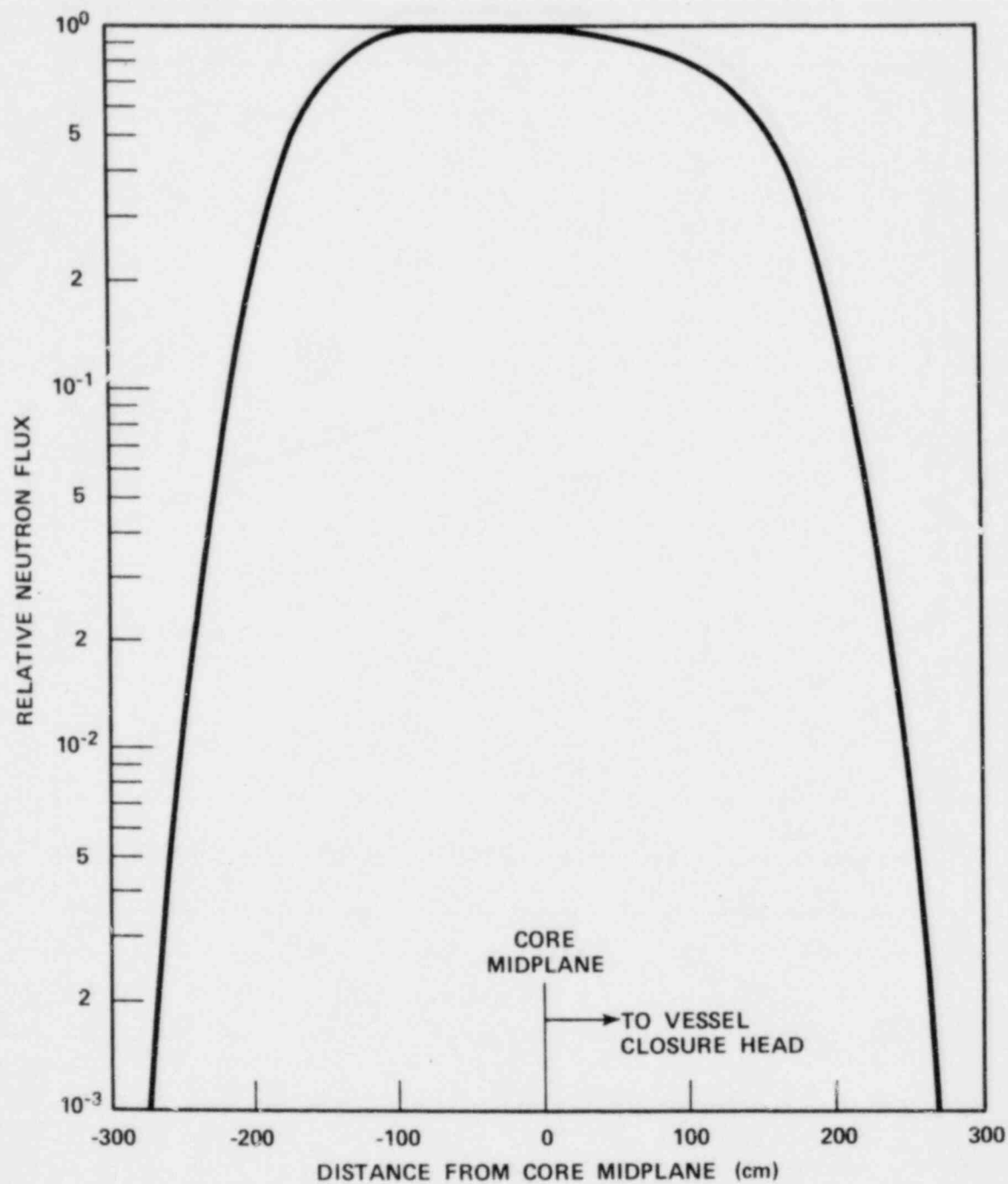


Figure 6-5. Relative Axial Variation of Fast Neutron Flux ($E > 1.0$ Mev) Within the Pressure Vessel

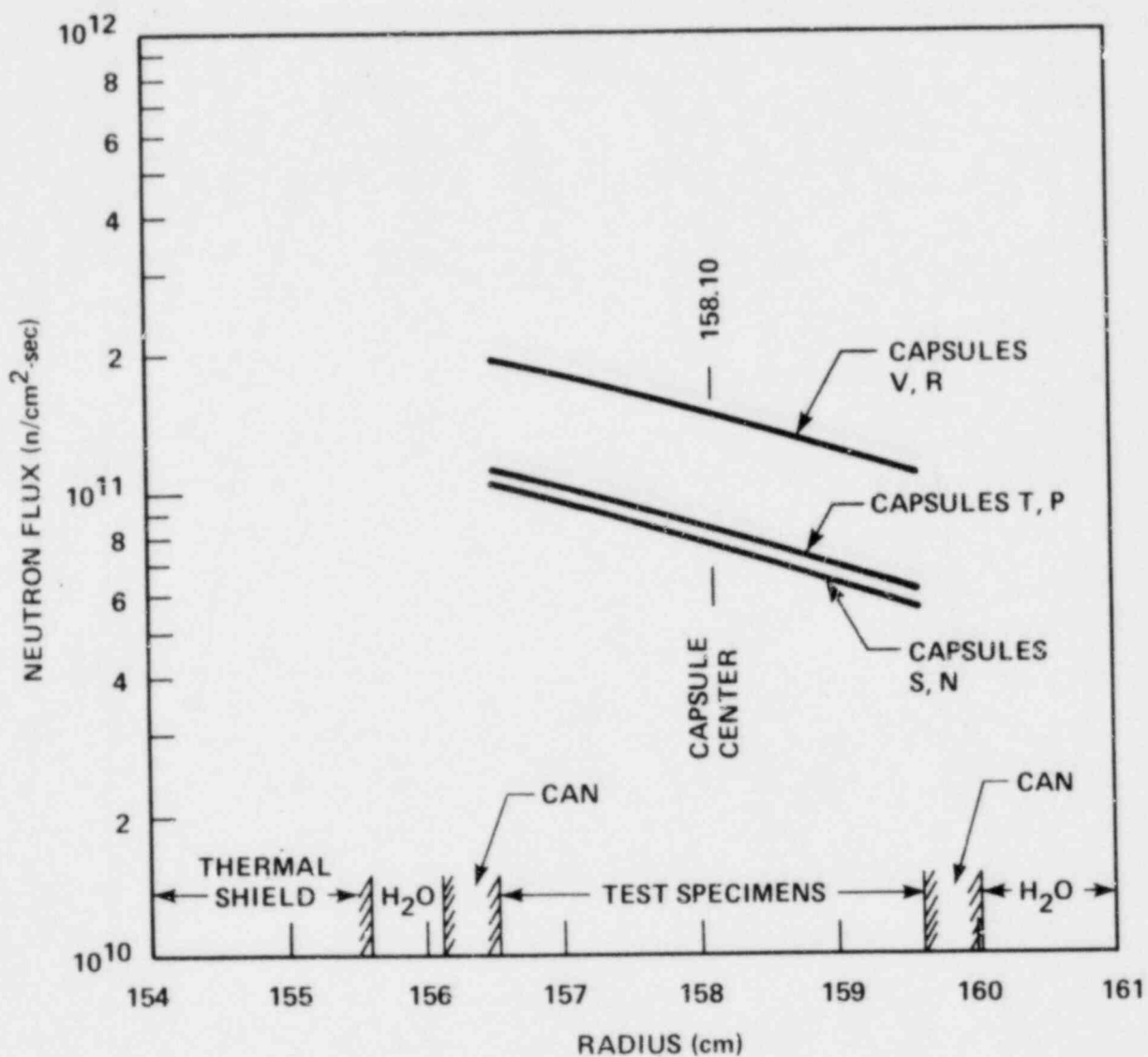


Figure 6-6. Calculated Radial Distribution of Maximum Fast Neutron Flux ($E > 1.0$ Mev) Within the Surveillance Capsules

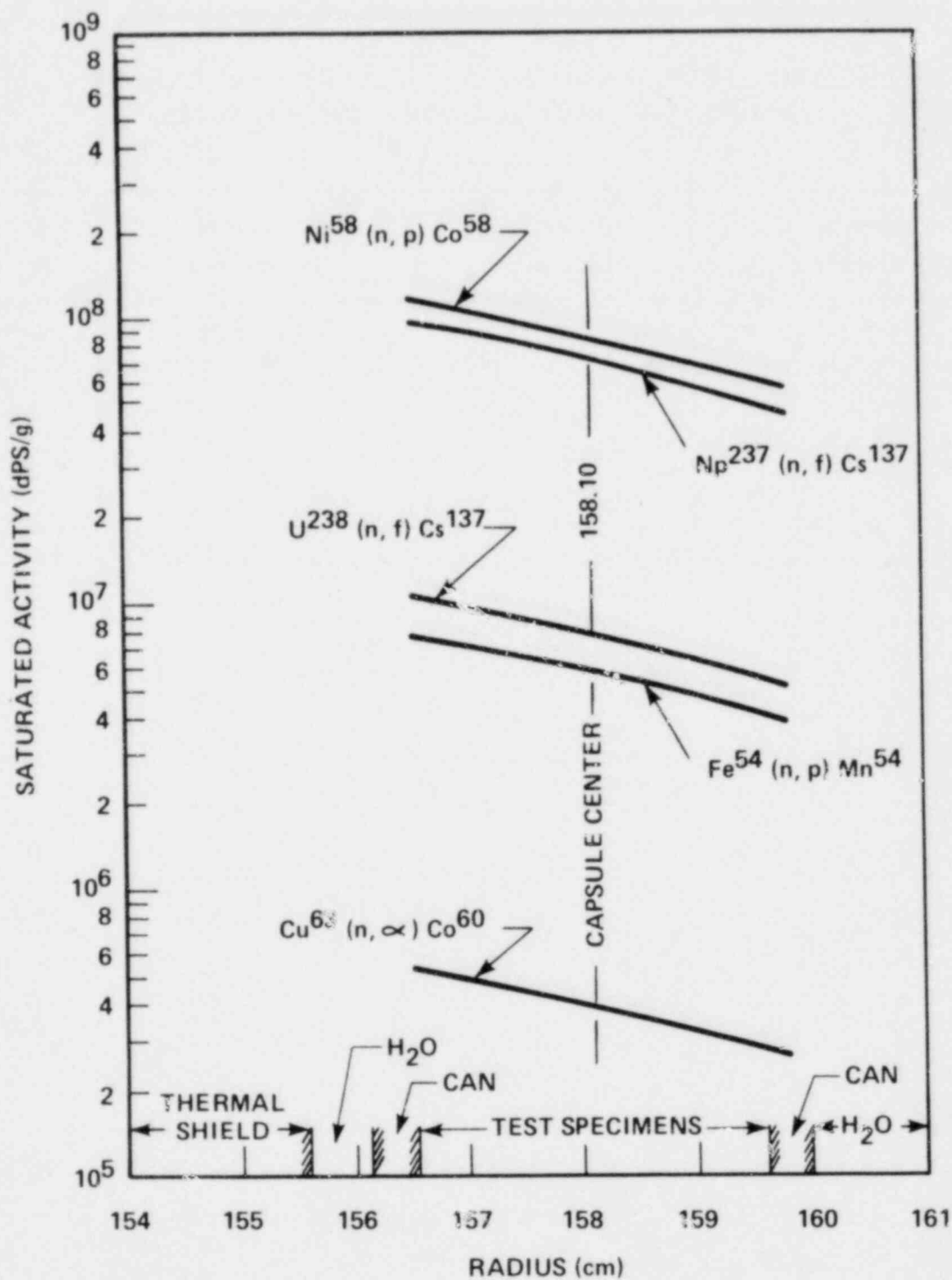


Figure 6-7. Calculated Variation of Fast Neutron Flux Monitor Saturated Activity Within Capsules V and R

TABLE 6-3

CALCULATED FAST NEUTRON FLUX ($E > 1.0$ Mev) AND LEAD
FACTORS FOR KEWAUNEE SURVEILLANCE CAPSULES

Capsule Identification	Azimuthal Location	ϕ ($E > 1.0$ Mev) (n/cm ² -sec)	Lead Factor
V	13°	1.45×10^{11}	3.37
R	13°	1.45×10^{11}	3.37
T	23°	8.33×10^{11}	1.94
P	23°	8.33×10^{10}	1.94
S	33°	7.67×10^{10}	1.79
N	33°	7.67×10^{10}	1.79

TABLE 6-4

CALCULATED NEUTRON ENERGY SPECTRA AT THE CENTER
OF KEWAUNEE SURVEILLANCE CAPSULES

Group No.	Capsules V and R	Neutron Flux (n/cm ² -sec)	
		Capsules T and P	Capsules S and N
1	8.17×10^8	5.99×10^8	5.26×10^8
2	2.68×10^9	1.99×10^9	1.75×10^9
3	4.43×10^9	3.08×10^9	2.73×10^9
4	4.98×10^9	3.18×10^9	2.89×10^9
5	8.66×10^9	5.20×10^9	4.75×10^9
6	1.70×10^{10}	1.01×10^{10}	9.26×10^9
7	2.46×10^{10}	1.41×10^{10}	1.30×10^{10}
8	3.53×10^{10}	1.97×10^{10}	1.83×10^{10}
9	4.67×10^{10}	2.53×10^{10}	2.35×10^{10}
10	5.04×10^{10}	2.67×10^{10}	2.48×10^{10}
11	1.67×10^{11}	8.66×10^{10}	8.03×10^{10}
12	2.11×10^{11}	1.05×10^{11}	9.76×10^{10}
13	9.42×10^{10}	4.65×10^{10}	4.34×10^{10}
14	7.11×10^{10}	3.52×10^{10}	3.28×10^{10}
15	5.67×10^{10}	2.80×10^{10}	2.62×10^{10}
16	1.32×10^{11}	6.41×10^{10}	5.99×10^{10}
17	1.03×10^{11}	5.07×10^{10}	4.73×10^{10}
18	1.06×10^{11}	5.14×10^{10}	4.82×10^{10}
19	8.41×10^{10}	4.09×10^{10}	3.83×10^{10}
20	9.34×10^{10}	4.52×10^{10}	4.23×10^{10}
21	2.97×10^{11}	1.51×10^{11}	1.36×10^{11}

TABLE 6-5

**SPECTRUM AVERAGED REACTION CROSS SECTIONS AT THE DOSIMETER
BLOCK LOCATION FOR KEWAUNEE SURVEILLANCE CAPSULES**

Reaction	$\bar{\sigma}$ (barns)		
	Capsules V and R	Capsules T and P	Capsules S and N
$\text{Fe}^{54}(\text{n,p})\text{Mn}^{54}$	0.0595	0.0683	0.0666
$\text{Ni}^{58}(\text{n,p})\text{Co}^{58}$	0.0811	0.0912	0.0893
$\text{Cu}^{63}(\text{n},\alpha)\text{Co}^{60}$	0.000404	0.000517	0.000494
$\text{U}^{238}(\text{n,f})\text{F.P.}$	0.333	0.345	0.344
$\text{Np}^{237}(\text{n,f})\text{F.P.}$	2.93	2.80	2.82

$$\bar{\sigma} = \frac{\int_0^{\infty} \sigma(E) \phi(E) dE}{\int_{1 \text{ Mev}}^{\infty} \phi(E) dE}$$

6-5. DOSIMETRY RESULTS

The irradiation history of the Kewaunee reactor is given in table 6-6. Comparisons of measured and calculated saturated activity of the flux monitors contained in Capsules V and R are listed in tables 6-7 and 6-8, respectively. The data are presented as measured at the actual monitor locations as well as adjusted to the capsule center. All adjustments to the capsule center were based on the data presented in figure 6-7.

As noted in reference 3, reaction rate ratios obtained from fast neutron dosimetry indicated that Capsule V had been rotated 180 degrees from the configuration shown in figure 6-2. Data from Capsule R, however, indicate that this capsule was inserted in the reactor with the orientation shown in figure 6-2. All adjustments to the capsule center were based on the assumption that Capsule V had been rotated while Capsule R had not.

TABLE 6-6

IRRADIATION HISTORY OF KEWAUNEE REACTOR VESSEL
SURVEILLANCE CAPSULES

Month	P _j (MW)	P _{max} (MW)	P _j /P _{max}	Irradiation Time (days)	Decay Time (days)
4/74	267	1650	.162	17	2364
5/74	790	1650	.479	31	2333
6/74	1201	1650	.728	30	2303
7/74	1160	1650	.703	31	2272
8/74	1582	1650	.959	31	2241
9/74	909	1650	.551	30	2211
10/74	419	1650	.254	31	2180
11/74	1018	1650	.617	30	2150
12/74	1165	1650	.706	31	2119
1/75	1008	1650	.611	31	2088
2/75	1350	1650	.818	28	2060
3/75	1432	1650	.868	31	2029
4/75	1107	1650	.671	30	1999
5/75	1107	1650	.671	31	1968
6/75	1021	1650	.619	30	1938
7/75	1091	1650	.661	31	1907
8/75	1523	1650	.923	31	1876
9/75	794	1650	.481	30	1846
10/75	1190	1650	.721	31	1815
11/75	1087	1650	.659	30	1785
12/75	1493	1650	.905	31	1754
1/76	1411	1650	.855	31	1723
2/76	1530	1650	.927	13	1710
Capsule V Removed					
2/76-	0	1650	.000	47	1663
3/76					
4/76	487	1650	.295	30	1633
5/76	904	1650	.548	31	1602
6/76	1591	1650	.964	30	1572
7/76	1543	1650	.935	31	1541
8/76	1558	1650	.944	31	1510
9/76	1437	1650	.871	30	1480
10/76	1576	1650	.955	31	1449
11/76	1546	1650	.937	30	1419
12/76	1551	1650	.940	31	1388

TABLE 6-6 (cont)

IRRADIATION HISTORY OF KEWAUNEE REACTOR VESSEL
SURVEILLANCE CAPSULES

Month	P_i (MW)	P_{max} (MW)	P_i/P_{max}	Irradiation Time (days)	Decay Time (days)
1/77	784	1650	.475	31	1357
2/77	0	1650	.000	28	1329
3/77	244	1650	.148	31	1298
4/77	1379	1650	.836	30	1268
5/77	1584	1650	.960	31	1237
6/77	1587	1650	.962	30	1207
7/77	1592	1650	.965	31	1176
8/77	1389	1650	.842	31	1145
9/77	1610	1650	.976	30	1115
10/77	1599	1650	.969	31	1084
11/77	1605	1650	.973	30	1054
12/77	1571	1650	.952	31	1023
1/78	1596	1650	.967	31	992
2/78	1582	1650	.959	28	964
3/78	1564	1650	.948	31	933
4/78	1092	1650	.662	30	903
5/78	85	1650	.0516	31	872
6/78	1373	1650	.832	30	842
7/78	1485	1650	.900	31	811
8/78	1539	1650	.933	31	790
9/78	1526	1650	.925	30	750
10/78	1577	1650	.956	31	719
11/78	1528	1650	.926	30	689
12/78	1569	1650	.951	31	658
1/79	1577	1650	.956	31	627
2/79	1505	1650	.912	28	599
3/79	1472	1650	.892	31	568
4/79	1538	1650	.932	30	538
5/79	1261	1650	.764	31	507
6/79-	0	1650	.000	61	446
7/79					
8/79	967	1650	.586	31	415
9/79	1538	1650	.932	30	385
10/79	1566	1650	.949	31	354
11/79	1599	1650	.969	30	324
12/79	1587	1650	.962	31	293

TABLE 6-6 (cont)

IRRADIATION HISTORY OF KEWAUNEE REACTOR VESSEL
SURVEILLANCE CAPSULES

Month	P_j (MW)	P_{max} (MW)	P_j/P_{max}	Irradiation Time (days)	Decay Time (days)
1/80	939	1650	.569	31	262
2/80	1647	1650	.998	29	234
3/80	1615	1650	.979	31	203
4/80	1591	1650	.964	30	173
5/80	1417	1650	.859	10	163

TABLE 6-7

**COMPARISON OF MEASURED AND CALCULATED FAST NEUTRON FLUX
MONITOR SATURATED ACTIVITIES FOR CAPSULE V**

Reaction and Axial Location	Radial Location (cm)	Saturated Activity (dis/s)		Adjusted Saturated Activity (dis/s)	
		Capsule V	Calculated	Capsule V	Calculated
$\text{Fe}^{54}_{(n,p)}\text{Mn}^{54}$					
Top	158.33	5.22×10^6	5.38×10^6	5.48×10^6	
Top-Middle	158.33	4.76×10^6	5.38×10^6	5.00×10^6	
Middle	158.33	4.98×10^6	5.38×10^6	5.23×10^6	
Bottom-Middle	158.33	4.93×10^6	5.38×10^6	5.18×10^6	
Bottom	158.33	5.36×10^6	5.38×10^6	5.63×10^6	
Average				5.30×10^6	5.65×10^6
$\text{Cu}^{63}_{(n,\alpha)}\text{Co}^{60}$					
Top-Middle	157.33	5.00×10^5	4.57×10^5	4.22×10^5	
Bottom-Middle	157.33	5.68×10^5	4.57×10^5	4.80×10^5	
Average				4.51×10^5	3.86×10^5
$\text{Ni}^{58}_{(n,p)}\text{Co}^{58}$					
Middle	157.33	8.55×10^7	9.84×10^7	7.27×10^7	8.37×10^7
$\text{Np}^{237}_{(n,f)}\text{Cs}^{137}$					
Middle	158.10	7.84×10^7	7.01×10^7	7.84×10^7	7.01×10^7
$\text{U}^{238}_{(n,f)}\text{Cs}^{137}$					
Middle	158.10	8.89×10^6	7.72×10^6	8.89×10^6	7.72×10^6

TABLE 6-8

COMPARISON OF MEASURED AND CALCULATED FAST NEUTRON FLUX
MONITOR SATURATED ACTIVITIES FOR CAPSULE R

Reaction and Axial Location	Radial Location (cm)	Saturated Activity (dis/s)		Adjusted Saturated Activity (dis/s)	
		Capsule R	Calculated	Capsule R	Calculated
Fe ⁵⁴ (n,p)Mn ⁵⁴					
Top	157.87	4.05 x 10 ⁶	5.92 x 10 ⁶	3.87 x 10 ⁶	
Top-Middle	157.87	3.76 x 10 ⁶	5.92 x 10 ⁶	3.59 x 10 ⁶	
Middle	157.87	3.80 x 10 ⁶	5.92 x 10 ⁶	3.63 x 10 ⁶	
Bottom	157.87	4.17 x 10 ⁶	5.92 x 10 ⁶	3.98 x 10 ⁶	
Average				3.77 x 10 ⁶	5.65 x 10 ⁶
Cu ⁶³ (n,γ)Co ⁶⁰	158.87	4.20 x 10 ⁵	3.28 x 10 ⁵	4.94 x 10 ⁵	3.86 x 10 ⁵
Ni ⁵⁸ (n,p)Co ⁵⁸					
Middle	158.87	7.23 x 10 ⁷	7.12 x 10 ⁷	8.50 x 10 ⁷	8.37 x 10 ⁷
Np ²³⁷ (n,f)Cs ¹³⁷					
Middle	158.10	not determined	7.01 x 10 ⁷	not determined	7.01 x 10 ⁷
U ²³⁸ (n,f)Cs ¹³⁷					
Middle	158.10	8.33 x 10 ⁶	7.72 x 10 ⁶	8.33 x 10 ⁶	7.72 x 10 ⁶

The fast neutron ($E > 1.0$ Mev) flux and fluence levels derived for Capsules V and R are presented in table 6-9. The thermal neutron flux obtained from the cobalt-aluminum monitors is summarized in table 6-10. Due to the relatively low thermal neutron flux at the capsule locations, no burnup correction was made to any of the measured activities. The maximum error introduced by this assumption is estimated to be less than 1 percent for the $\text{Ni}^{58} (n,p) \text{Co}^{58}$ reaction and even less significant for all of the other fast neutron reactions.

Using the average measured data from all of the fast neutron dosimetry presented in table 6-9 along with the lead factors given in table 6-3, the fast neutron fluences ($E > 1.0$ Mev) for Capsules V and R as well as for the reactor vessel inner diameter are summarized in table 6-11 and figure 6-8. The agreement between calculation and measurement is excellent, with measured fluence levels of 5.99×10^{18} and $2.07 \times 10^{19} \text{ n/cm}^2$ compared to calculated values of 5.71×10^{18} and $2.06 \times 10^{19} \text{ n/cm}^2$ for Capsules V and R, respectively. Further, the graphical representation in figure 6-8 indicates the accuracy of the transport analysis for Kewaunee and supports the use of the analytically determined fluence trend curve for predicting vessel toughness at times in the future.

It should be noted that Westinghouse normally uses $\text{Fe}^{54} (n,p) \text{Mn}^{54}$ measured results to quote capsule exposures. However, the iron data obtained from Capsule R are inconsistent with the remaining dosimetry from Capsule R as well as with iron data from Capsule V. From table 6-11, it is seen that the iron data from Capsule V agree with the overall average within 12 percent while for Capsule R the iron data are low by 51 percent. The reason for this discrepancy is not known. However, it is believed that the average measured fluence is a better indicator of Capsule R exposure than are the $\text{Fe}^{54} (n,p) \text{Mn}^{54}$ data.

Projecting to end-of-life, a summary of peak fast neutron exposure of the Kewaunee reactor as derived from both calculation and measurement may be made as follows.

	Fast Neutron Fluence (n/cm^2)		
	Surface	1/4 T	3/4 T
Capsule V	4.56×10^{19}	2.97×10^{19}	8.96×10^{18}
Capsule R	4.37×10^{19}	2.85×10^{19}	8.59×10^{18}
Avg Measurement	4.47×10^{19}	2.91×10^{19}	8.78×10^{18}
Calculation	4.34×10^{19}	2.83×10^{19}	8.53×10^{18}

These data are based on 32 full power years of operation at 1650 MWt.

TABLE 6-9

RESULTS OF FAST NEUTRON DOSIMETRY FOR CAPSULES V AND R

Capsule	Reaction	Adjusted Saturated Activity (dis/s)		ϕ (E > 1.0 Mev) (n/cm ² -sec)		ϕ (E > 1.0 Mev) (n/cm ²)	
		Measured	Calculated	Measured	Calculated	Measured	Calculated
V	Fe ⁵⁴ (n,p)Mn ⁵⁴	5.30 x 10 ⁶	5.65 x 10 ⁶	1.36 x 10 ¹¹	1.45 x 10 ¹¹	5.36 x 10 ¹⁸	5.71 x 10 ¹⁸
	Cu ⁶³ (n, α)Co ⁶⁰	4.51 x 10 ⁵	3.86 x 10 ⁵	1.69 x 10 ¹¹		6.66 x 10 ¹⁸	
	Ni ⁵⁸ (n,p)Co ⁵⁸	7.27 x 10 ⁷	8.37 x 10 ⁷	1.26 x 10 ¹¹		4.96 x 10 ¹⁸	
	Np ²³⁷ (n,f)Cs ¹³⁷	7.84 x 10 ⁷	7.01 x 10 ⁷	1.52 x 10 ¹¹		6.38 x 10 ¹⁸	
	U ²³⁸ (n,f)Cs ¹³⁷	8.89 x 10 ⁶	7.72 x 10 ⁶	1.67 x 10 ¹¹		6.58 x 10 ¹⁸	
R	Fe ⁵⁴ (n,p)Mn ⁵⁴	3.77 x 10 ⁶	5.65 x 10 ⁶	9.68 x 10 ¹⁰	1.45 x 10 ¹¹	1.37 x 10 ¹⁹	2.06 x 10 ¹⁹
	Cu ⁶³ (n, α)Co ⁶⁰	4.94 x 10 ⁵	3.86 x 10 ⁵	1.86 x 10 ¹¹		2.64 x 10 ¹⁹	
	Ni ⁵⁸ (n,p)Co ⁵⁸	8.50 x 10 ⁷	8.37 x 10 ⁷	1.47 x 10 ¹¹		2.09 x 10 ¹⁹	
	Np ²³⁷ (n,f)Cs ¹³⁷	not determined	7.01 x 10 ⁷	not determined		—	
	U ²³⁸ (n,f)Cs ¹³⁷	8.33 x 10 ⁶	7.72 x 10 ⁶	1.56 x 10 ¹¹		2.22 x 10 ¹⁹	

TABLE 6-10

RESULTS OF THERMAL NEUTRON DOSIMETRY FOR CAPSULES V AND R

Capsule	Axial Location	Saturated Activity (dis/s)		ϕ_{th} (n/cm ² -sec)
		Bare	Cd Covered	
V	top	1.65×10^8	7.33×10^7	1.62×10^{11}
	bottom	not determined	7.40×10^7	not determined
R	top	1.35×10^8	6.70×10^7	1.20×10^{11}
	bottom	1.42×10^8	6.01×10^7	1.44×10^{11}

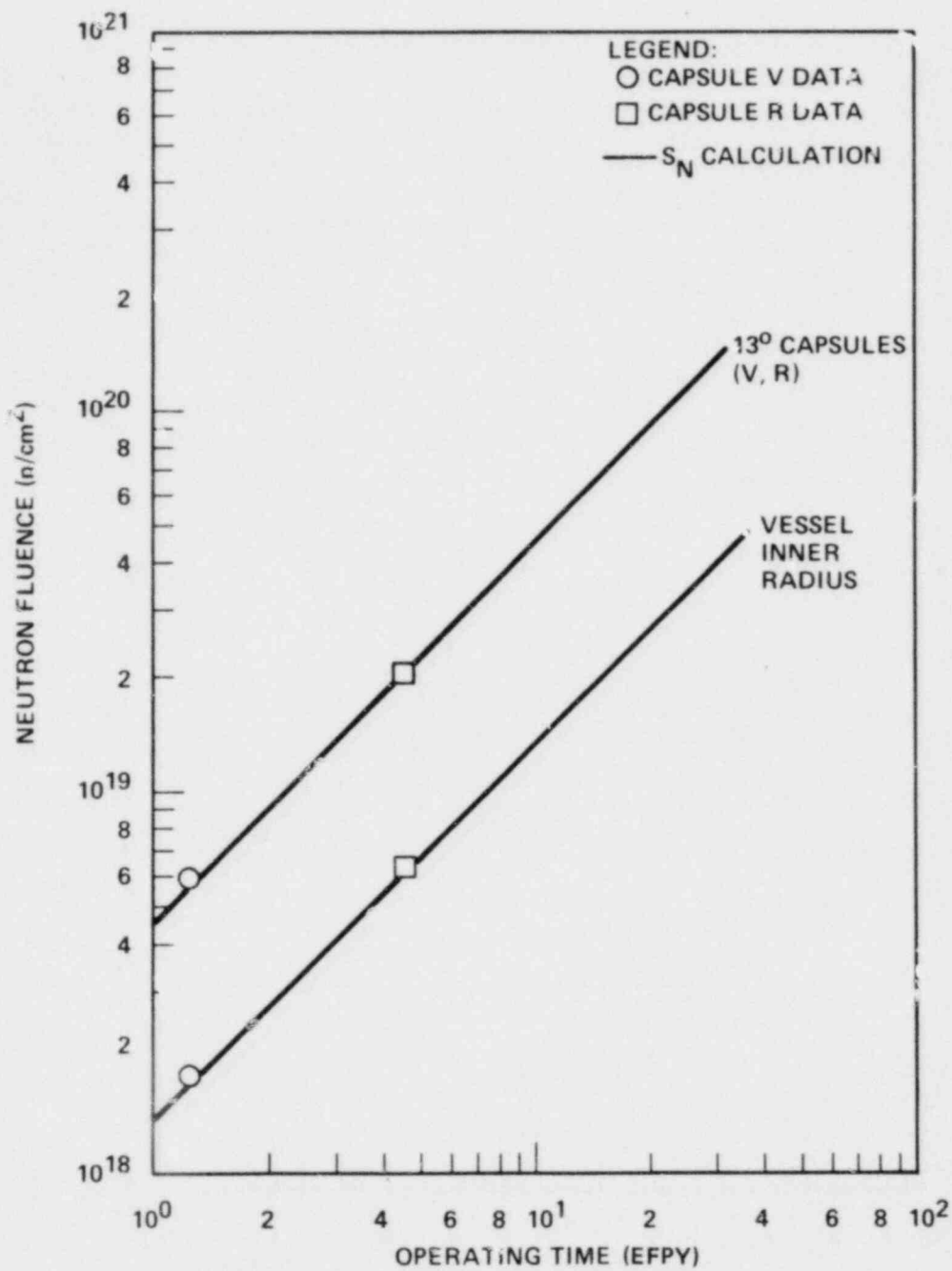


Figure 6-8. Comparison of Measured and Calculated Fast Neutron Fluence ($E > 1.0$ Mev) for Capsules V and R

TABLE 6-11

SUMMARY OF FAST NEUTRON DOSIMETRY RESULTS FOR CAPSULES V AND R

Capsule	Irradiation Time (EFPS)	ϕ ($E > 1.0$ Mev) ($n/cm^2 \cdot sec$)	ϕ ($E > 1.0$ Mev) (n/cm^2)	Lead Factor	Vessel Fluence (n/cm^2)	Calculated Vessel Fluence (n/cm^2)
Based on the $Fe^{54} (n,p) Mn^{54}$ Reaction						
V	3.94×10^7	1.36×10^{11}	5.36×10^{18}	3.37	1.59×10^{18}	1.69×10^{18}
R	1.42×10^8	9.68×10^{10}	1.37×10^{19}	3.37	4.54×10^{18}	6.11×10^{18}
Based on the Average of All Fast Neutron Reactions						
V	3.94×10^7	1.52×10^{11}	5.99×10^{18}	3.37	1.78×10^{18}	1.69×10^{18}
R	1.42×10^8	1.46×10^{11}	2.07×10^{19}	3.37	6.14×10^{18}	6.11×10^{18}

Based on the fluence measurements for Capsule R, the vessel 1/4 thickness fluence after 4.5 effective full power years of operations is $3.77 \times 10^{18} \text{ n/cm}^2$ compared to a calculated fluence of $3.75 \times 10^{18} \text{ n/cm}^2$.

Based on the new capsule to vessel inner wall lead factors identified in table 6-3 and the new capsule withdrawal schedule identified in ASTM E185-79, it is recommended that future capsules be removed from the reactor in accordance with the following schedule:

Capsule Identity	Vessel Location	Lead Factor	Removal Time	Capsule Fluence (n/cm ²)
V	77°	3.37	1.25 EFPY (removed)	5.99×10^{18}
R	257°	3.37	4.50 EFPY (removed)	2.07×10^{19}
T	67°	1.94	11.00 EFPY	2.89×10^{19} [a]
P	247°	1.94	16.00 EFPY	4.21×10^{19} [b]
S	57°	1.79	32.00 EFPY	8.42×10^{19}
M	237°	1.79	Standby	—

a. Represents approximate EOL fluence at the vessel 1/4 thickness

b. Represents approximate EOL fluence at the vessel inside surface

REFERENCES

1. Yanichko, S. E., D. J. Lege, and G. C. Zula, "Wisconsin Public Service Corp. Kewaunee Nuclear Power Plant Reactor Vessel Radiation Surveillance Program" WCAP-8107, April 1973.
2. ASTM Designation E185-70 "Surveillance Tests for Nuclear Reactor Vessels" in ASTM Standard (1971) Part 31, American Society for Testing and Materials, Philadelphia, Pa., 1971.
3. Yanichko, S. E., S. L. Anderson, and K. V. Scott, "Analysis of Capsule V from the Wisconsin Public Service Corporation Kewaunee Nuclear Plant Reactor Vessel Radiation Surveillance Program," WCAP-8908, January 1977.
4. Regulatory Guide 1.99, Revision 1, "Effects of Residual Elements on Predicted Radiation Damage to Reactor Vessel Materials," U.S. Nuclear Regulatory Commission, April 1977.
5. Soltesz, R. G., R. K. Disney, J. Jedruch, and S. L. Zeigler, "Nuclear Rocket Shielding Methods, Modification, Updating and Input Data Preparation — Volume 5 — Two-Dimensional, Discrete Ordinates Transport Technique," WANL-PR-(LL)-034, Vol. 5, August 1970.
6. Collier, G., G. Gibson, L. L. Moran, R. K. Disney, and R. S. Kaiser, "Second Version of the GAMBIT Code, WANL-TME-1969, November 1969.
7. Soltesz, R. G., R. K. Disney, S. L. Zeigler, "Nuclear Rocket Shielding Methods, Modification, Updating and Input Data Preparation — Volume 3, Cross-Section Generation and Data Processing Techniques," WANL-PR-(LL)-034, August 1970.
8. Soltesz, R. G. and R. K. Disney, "Nuclear Rocket Shielding Methods, Modification, Updating and Input Data Preparation — Volume 4 — One-Dimensional Discrete Ordinates Transport Technique," WANL-PR-(LL)-034, August 1970.
9. ASTM Designation E261-70, Standard Method for Measuring Neutron Flux by Radioactivation Techniques," in ASTM Standards (1975), Part 45, Nuclear Standards, pp. 745-755, American Society for Testing and Materials, Philadelphia, Pa., 1975.
10. ASTM Designation E262-70, "Standard Method for Measuring Thermal Neutron Flux by Radioactivation Techniques," in ASTM Standards (1975), Part 45, Nuclear Standards, pp. 756-763, American Society for Testing and Materials, Philadelphia, Pa., 1975.
11. ASTM Designation E263-70, "Standard Method for Measuring Fast-Neutron Flux by Radioactivation of Iron," in ASTM Standards (1975), Part 45, Nuclear Standards, pp. 764-769, American Society for Testing and Materials, Philadelphia, Pa., 1975.

12. ASTM Designation E481-73T, "Tentative Method of Measuring Neutron-Flux Density by Radioactivation of Cobalt and Silver," in ASTM Standards (1975), Part 45, Nuclear Standards, pp. 887-894, American Society for Testing and Materials, Philadelphia, Pa., 1975.
13. ASTM Designation E264-70, "Standard Method for Measuring Fast-Neutron Flux by Radioactivation of Nickel," in ASTM Standards (1975), Part 45, Nuclear Standards, pp. 770-774, American Society for Testing and Materials, Philadelphia, Pa., 1975.
14. Anderson, S. L., "Characterization of the Neutron Environment for Commercial LWR Pressure Vessel Surveillance Programs" in Proceedings of the Second ASTM-EUROTOM Symposium on Reactor Dosimetry, NUREG/CP-0004, October 1977, Vol. 3, pp. 1093-1107.